

# Smoothing and Decomposition for Analysis Sparse Recovery

Zhao Tan, *Student Member, IEEE*, Yonina C. Eldar, *Fellow, IEEE*,  
Amir Beck, and Arye Nehorai, *Fellow, IEEE*

## Abstract

We consider algorithms and recovery guarantees for the analysis sparse model where the signal is sparse with respect to a highly coherent frame. We first consider the use of the monotone version of the fast iterative shrinkage-thresholding algorithm (MFISTA) to solve the analysis sparse recovery problem. Since the proximal operator in MFISTA does not have a closed-form solution for the analysis model, it cannot be applied directly. Instead, we examine two alternatives based on smoothing and decomposition transformations that relax the original sparse recovery problem, and then implement MFISTA on the relaxed formulation. We refer to these two methods as smoothing-based MFISTA and decomposition-based MFISTA. We analyze the convergence of both algorithms, and establish that smoothing-based MFISTA converges more rapidly when applied to general nonsmooth optimization problems. We then derive a performance bound on the reconstruction error using these algorithms. The bound proves that our methods can recover a sparse signal in terms of a redundant tight frame when the measurement matrix satisfies a properly adapted restricted isometry property. Extensive numerical examples demonstrate the performance of our algorithms and show that smoothing-based MFISTA converges faster than the decomposition-based alternative in real applications, such as CT image reconstruction.

## Index Terms

Analysis model, sparse recovery, fast iterative shrinkage-thresholding algorithm, smoothing and decomposition, convergence analysis, restricted isometry property.

Z. Tan and A. Nehorai are with the Preston M. Green Department of Electrical and Systems Engineering Department, Washington University in St. Louis, St. Louis, MO, 63130 USA. E-mail: {tanz, nehorai}@ese.wustl.edu.

Y. C. Eldar is with the Department of Electrical Engineering, Technion—Israel Institute of Technology, Haifa 32000, Isreal. E-mail: yonina@ee.technion.ac.il.

A. Beck is with the Department of Industrial Engineering and Management, Technion—Israel Institute of Technology, Haifa 32000, Isreal. E-mail: becka@ee.technion.ac.il.

The work of Z. Tan and A. Nehorai was supported by the AFOSR Grant FA9550-11-1-0210, NSF Grant CCF-1014908, and ONR Grant N000141310050. The work of Y. C. Eldar was supported in part by the Israel Science Foundation under Grant no. 170/10, in part by the Ollendorf Foundation, in part by a Magnet grant Metro450 from the Israel Ministry of Industry and Trade, and in part by the Intel Collaborative Research Institute for Computational Intelligence (ICRI-CI). The work of A. Beck was partially supported by the Israel Science Foundation under grant ISF No.253/12.

## I. INTRODUCTION

Low-dimensional signal recovery exploits the fact that many natural signals are inherently low dimensional, although they may have high ambient dimension. Prior information about the low-dimensional space can be explored to aid in recovery of a signal of interest. Signal sparsity is one of the popular forms of prior information, and is the prior that underlies the growing field of compressive sensing [1]-[4]. Recovery of sparse inputs has found many applications in areas such as imaging, speech, radar signal processing, sub-Nyquist sampling and more. A typical sparse recovery problem has the following linear form:

$$(M) \quad \mathbf{y} = \mathbf{A}\mathbf{x} + \mathbf{w},$$

in which  $\mathbf{A} \in \mathbb{R}^{m \times n}$  is a measurement matrix,  $\mathbf{y} \in \mathbb{R}^m$  is the measurement vector, and  $\mathbf{w} \in \mathbb{R}^m$  is the noise term. Our goal is to recover the signal  $\mathbf{x} \in \mathbb{R}^n$ . Normally we have  $m < n$ , which indicates that the inverse problem is ill-posed and has an infinite number of solutions. To find a unique solution prior information on  $\mathbf{x}$  must be incorporated.

In the synthesis approach it is assumed that  $\mathbf{x}$  can be expressed as a sparse combination of known dictionary elements. That is,  $\mathbf{x} = \mathbf{D}\boldsymbol{\alpha}$ ,  $\mathbf{D} \in \mathbb{R}^{n \times p}$ , with  $\boldsymbol{\alpha}$  sparse, i.e., the number of non-zero elements in  $\boldsymbol{\alpha}$  is far less than the length of  $\boldsymbol{\alpha}$ . This approach is well-developed including efficient numerical algorithms and recovery guarantees. The main methods for solving this problem can be classified into two categories. One includes greedy methods, such as iterative hard thresholding [5] and orthogonal matching pursuit [6]. The other is based on relaxation-type methods, such as basis pursuit [7] and LASSO [8]. These algorithms can stably recover a sparse signal  $\boldsymbol{\alpha}$  when the matrix  $\mathbf{A}\mathbf{D}$  satisfies the restricted isometry property (RIP) [9]-[11].

Recently, an alternative approach has become popular, which is known as the analysis method [12], [13]. In this framework, we are given an analysis dictionary  $\mathbf{D}^*$  ( $\mathbf{D} \in \mathbb{R}^{n \times p}$ ) under which  $\mathbf{D}^*\mathbf{x}$  is sparse. Assuming, for example, that the  $\ell_2$  norm of the noise  $\mathbf{w}$  is bounded by  $\varepsilon$ , the recovery problem can be formulated as

$$\min_{\mathbf{x} \in \mathbb{R}^n} \|\mathbf{D}^*\mathbf{x}\|_0 \quad \text{subject to } \|\mathbf{y} - \mathbf{A}\mathbf{x}\|_2 \leq \varepsilon.$$

Since this problem is NP hard, several greedy algorithms have been proposed to approximate it, such as thresholding [14] and subspace pursuit [15]. Alternatively, the nonconvex  $\ell_0$  norm can be approximated by the convex  $\ell_1$  norm leading to the following relaxed problem:

$$\min_{\mathbf{x} \in \mathbb{R}^n} \|\mathbf{D}^*\mathbf{x}\|_1 \quad \text{subject to } \|\mathbf{y} - \mathbf{A}\mathbf{x}\|_2 \leq \varepsilon. \quad (1)$$

We refer to this optimization problem as analysis basis pursuit (ABP), and note that it is equivalent to the unconstrained optimization

$$\min_{\mathbf{x} \in \mathbb{R}^n} \frac{1}{2} \|\mathbf{y} - \mathbf{A}\mathbf{x}\|_2^2 + \lambda \|\mathbf{D}^*\mathbf{x}\|_1, \quad (2)$$

which we call analysis LASSO (ALASSO). The equivalence is in the sense that for any  $\varepsilon > 0$  there exists a  $\lambda$  for which the optimal solutions of ABP and ALASSO are identical.

Both optimizations ABP and ALASSO can be solved using interior point methods [16]. However, when the problem dimension grows, these techniques become very slow since they require solutions of linear systems. Another suggested approach is based on alternating direction method of multipliers (ADMM) [17], [18]. The efficiency of this method highly depends on nice structure of the matrix  $\mathbf{A}$ . First-order algorithms, such as the fast iterative shrinkage-thresholding algorithm (FISTA), are more favorable in dealing with large dimensional data since it does not require  $\mathbf{A}$  to have any structure. However, FISTA is not a monotone algorithm, i.e., the objective function values are not guaranteed to be non-increasing. In this paper, we consider a monotone version of FISTA, which is also known as MFISTA in the literature [19]. The difficulty in directly applying first-order techniques to ABP and ALASSO is the nonsmooth term  $\|\mathbf{D}^*\mathbf{x}\|_1$  in the objective function. Several prior works [20], [21] have considered nonsmooth optimization problems and treated them by transforming the nondifferentiable problem into a smooth counterpart. For example, in [21], the authors used Nesterov’s smoothing-based method [22] in conjunction with continuation (NESTA) to solve ABP. They considered ABP under the assumption that the matrix  $\mathbf{A}^*\mathbf{A}$  is an orthogonal projector. To avoid imposing conditions on  $\mathbf{A}$ , we focus in this paper on the ALASSO formulation.

It was shown in [20] that one can apply any fast first-order method, namely iterations that achieve an  $\varepsilon$ -optimal solution within  $O(\frac{1}{\sqrt{\varepsilon}})$  iterations, to an  $\varepsilon$  smooth-approximation of the problem and obtain an algorithm with  $O(\frac{1}{\varepsilon})$  iterations. Here we apply this smoothing approach together with MFISTA leading to the smoothing-based MFISTA (SFISTA) algorithm. We also propose a decomposition-based MFISTA method (DFISTA) to solve the analysis sparse recovery problem. The idea is to introduce an auxiliary variable  $\mathbf{z}$  and replace the term  $\|\mathbf{D}^*\mathbf{x}\|_1$  by  $\|\mathbf{z}\|_1 + \frac{\rho}{2}\|\mathbf{z} - \mathbf{D}^*\mathbf{x}\|_2^2$  for some  $\rho$ . In this formulation MFISTA can be applied in a simple and explicit manner. This decomposition approach can be traced back to [23], and has been widely used for solving total variation problems in the context of image reconstruction [24].

Both smoothing and decomposition based algorithms for nonsmooth optimization problems are very popular in the literature. One of the main goals of this paper is to examine their respective performance, and analyze which method is preferable. Our results are general, and are not restricted to the analysis sparse recovery problem. In the context of analysis sparse recovery, we show in Section II-C that both algorithms solve the following optimization problem:

$$\min_{\mathbf{x} \in \mathbb{R}^n, \mathbf{z} \in \mathbb{R}^p} \frac{1}{2}\|\mathbf{A}\mathbf{x} - \mathbf{b}\|_2^2 + \lambda\|\mathbf{z}\|_1 + \frac{1}{2}\rho\|\mathbf{z} - \mathbf{D}^*\mathbf{x}\|_2^2,$$

which we refer to as relaxed ALASSO (RALASSO). However, the solution methods are quite different, leading to different convergence behavior. For general nonsmooth convex optimization problems, the computational complexity of each iteration is the same for SFISTA and DFISTA. However, we prove that SFISTA requires fewer iterations to reach a predetermined accuracy.

Another contribution of this paper is in proving recovery guarantees for analysis sparse recovery using RALASSO. Previous work [12] studied recovery guarantees based on ABP and showed that if  $\mathbf{A}$  satisfies the  $2s$ -restricted isometry property adapted to  $\mathbf{D}$  (D-RIP) [12] with  $\sigma_{2s} \leq 0.08$ , and the  $\ell_2$  norm of the noise  $\mathbf{w}$  is bounded by a

constant  $\varepsilon$ , then the optimal solution  $\mathbf{x}_{\text{opt}}$  of (1) recovers  $\mathbf{x}$  with error bound:

$$\|\mathbf{x}_{\text{opt}} - \mathbf{x}\|_2 \leq C_0\varepsilon + C_1 \frac{\|\mathbf{D}^*\mathbf{x} - (\mathbf{D}^*\mathbf{x})_s\|_1}{\sqrt{s}}. \quad (3)$$

Here  $C_0$  and  $C_1$  are constants, and we use  $(\mathbf{x})_s$  to denote the vector consisting of the largest  $s$  entries of  $|\mathbf{x}|$ . This result was later improved in [25] by establishing that (3) holds with  $\sigma_{2s} \leq 0.493$ . In [26], a similar guarantee is developed for ALASSO (2) under the condition that  $\|\mathbf{D}^*\mathbf{A}^*\mathbf{w}\|_\infty \leq \frac{\lambda}{2}$ , and the D-RIP of  $\mathbf{A}$  satisfies  $\sigma_{3s} < 0.25$ , which is equivalent to  $\sigma_{2s} < 0.0833$  according to Corollary 3.4 in [27]. In this case the solution  $\mathbf{x}_{\text{opt}}$  of ALASSO satisfies

$$\|\mathbf{x}_{\text{opt}} - \mathbf{x}\|_2 \leq C_0\sqrt{s}\lambda + C_1 \frac{\|\mathbf{D}^*\mathbf{x} - (\mathbf{D}^*\mathbf{x})_s\|_1}{\sqrt{s}}, \quad (4)$$

where  $C_0, C_1$  are constants.

Here we combine the techniques in [9] and [26], and obtain a performance bound on RALASSO. We show that when  $\sigma_{2s} < 0.1907$  and  $\|\mathbf{D}^*\mathbf{A}^*\mathbf{w}\|_\infty \leq \frac{\lambda}{2}$ , the solution  $\mathbf{x}_{\text{opt}}$  of RALASSO satisfies

$$\|\mathbf{x}_{\text{opt}} - \mathbf{x}\|_2 \leq C_0\sqrt{s}\lambda + C_1 \frac{\|\mathbf{D}^*\mathbf{x} - (\mathbf{D}^*\mathbf{x})_s\|_1}{\sqrt{s}} + C_2 \frac{\lambda p}{\sqrt{s\rho}},$$

where  $p$  is the number of rows in  $\mathbf{D}^*$  and  $C_0, C_1, C_2$  are constants. As a special case, choosing  $\rho \rightarrow \infty$  shows that the bound in (4) holds for ALASSO as long as  $\sigma_{2s} < 0.1907$ , which improves upon the results of [26].

The paper is organized as follows. In Section II, we introduce some mathematical preliminaries, and present SFISTA and DFISTA for solving RALASSO. We analyze the convergence behavior of these two algorithms in Section III, and show that SFISTA converges faster than DFISTA. Performance guarantees on RALASSO are developed in Section IV. Finally, in Section V we test our techniques on two simulations: randomly generated data and CT image reconstruction. These numerical experiments demonstrate the effectiveness of our algorithms in solving the analysis recovery problem, and show that SFISTA performs favorably in comparison with DFISTA. A continuation method is also introduced to further accelerate the convergence speed.

Throughout the paper, we use capital italic bold letters to represent matrices and lowercase italic bold letters to represent vectors. For a given matrix  $\mathbf{D}$ ,  $\mathbf{D}^*$  denotes the matrix. For a matrix  $\mathbf{D}^*$ , we denote by  $\mathbf{D}_{\mathcal{T}}^*$  the matrix that maintains the rows in  $\mathbf{D}^*$  with indices in set  $\mathcal{T}$ , while setting all other rows to zero. Given a vector  $\mathbf{x}$ ,  $\|\mathbf{x}\|_1$ ,  $\|\mathbf{x}\|_2$  are the  $\ell_1, \ell_2$  norms respectively,  $\|\mathbf{x}\|_0$  is the  $\ell_0$  norm which counts the number of nonzero components, and  $\|\mathbf{x}\|_\infty$  denotes the maximum absolute value of elements in  $\mathbf{x}$ . We use  $\mathbf{x}[i]$  to represent the  $i$ th element of  $\mathbf{x}$ . For a matrix  $\mathbf{A}$ ,  $\|\mathbf{A}\|_2$  is the induced spectral norm, and  $\|\mathbf{A}\|_{p,q} = \max \frac{\|\mathbf{A}\mathbf{x}\|_p}{\|\mathbf{x}\|_q}$ . Finally,  $\text{Re}\langle \mathbf{a}, \mathbf{b} \rangle = \frac{\langle \mathbf{a}, \mathbf{b} \rangle + \langle \mathbf{b}, \mathbf{a} \rangle}{2}$ .

## II. SMOOTHING AND DECOMPOSITION FOR ANALYSIS SPARSE RECOVERY

In this section we present the smoothing-based and decomposition-based methods for solving the ALASSO problem. To do so, we first recall in Subsection II-A some results related to proximal gradient methods that will be essential to our presentation and analysis.

### A. The Proximal Gradient Method

We begin this section with the definition of Moreau’s proximal (or “prox”) operator [28], which is the key step in defining the proximal gradient method.

Given a closed proper convex function  $h : \mathbb{R}^n \rightarrow \mathbb{R} \cup \{\infty\}$ , the proximal operator of  $h$  is defined by

$$\text{prox}_h(\mathbf{x}) = \arg \min_{\mathbf{u} \in \mathbb{R}^n} \left\{ h(\mathbf{u}) + \frac{1}{2} \|\mathbf{u} - \mathbf{x}\|_2^2 \right\}.$$

The proximal operator can be computed efficiently in many important instances. For example, the proximal mapping can be easily obtained when  $h$  is an  $l_p$  norm ( $p \in [1, \infty)$ ), or an indicator of “simple” closed convex sets such as the box, unit-simplex and the ball. More examples of proximal operators as well as a wealth of properties can be found, for example, in [29].

The proximal operator can be used in order to compute smooth approximations of convex functions. Specifically, let  $h$  be a closed, proper, convex function, and let  $\mu > 0$  be a given parameter. Define

$$h_\mu(\mathbf{x}) = \min_{\mathbf{u} \in \mathbb{R}^n} \left\{ h(\mathbf{u}) + \frac{1}{2\mu} \|\mathbf{u} - \mathbf{x}\|_2^2 \right\}.$$

It is easy to see that

$$h_\mu(\mathbf{x}) = h(\text{prox}_{\mu h}(\mathbf{x})) + \frac{1}{2\mu} \|\mathbf{x} - \text{prox}_{\mu h}(\mathbf{x})\|_2^2.$$

The function  $h_\mu$  is called the *Moreau envelope of  $h$*  and has the following important properties (see [28] for further details):

- $h_\mu(\mathbf{x}) \leq h(\mathbf{x})$ .
- $h_\mu$  is continuously differentiable and its gradient is Lipschitz continuous with constant  $1/\mu$ .
- The gradient of  $h_\mu$  is given by

$$\nabla h_\mu(\mathbf{x}) = \frac{1}{\mu} (\mathbf{x} - \text{prox}_{\mu h}(\mathbf{x})). \quad (5)$$

One important usage of the proximal operator is in the proximal gradient method that is aimed at solving the following composite problem:

$$\min_{\mathbf{x} \in \mathbb{R}^n} \{F(\mathbf{x}) + G(\mathbf{x})\}. \quad (6)$$

Here  $F : \mathbb{R}^n \rightarrow \mathbb{R}$  is a continuously differentiable convex function with a continuous gradient that has Lipschitz constant  $L_{\nabla F}$ :

$$\|\nabla F(\mathbf{x}) - \nabla F(\mathbf{y})\|_2 \leq L_{\nabla F} \|\mathbf{x} - \mathbf{y}\|_2, \quad \text{for all } \mathbf{x}, \mathbf{y} \in \mathbb{R}^n,$$

and  $G : \mathbb{R}^n \rightarrow \mathbb{R} \cup \{\infty\}$  is an extended-valued, proper, closed and convex function. The *proximal gradient method* for solving (6) takes the following form (see [29], [30], [31]):

---

### Proximal Gradient Method For Solving (6)

---

**Input:** An upper bound  $L \geq L_{\nabla F}$ .

**Step 0.** Take  $\mathbf{x}_0 \in \mathbb{R}^n$ .

**Step k.** ( $k \geq 1$ )

$$\text{Compute } \mathbf{x}_k = \text{prox}_{\frac{1}{L}G} \left( \mathbf{x}_{k-1} - \frac{1}{L} \nabla F(\mathbf{x}_{k-1}) \right).$$


---

The main disadvantage of the proximal gradient method is that it suffers from a relatively slow  $O(1/k)$  rate of convergence of the function values. An accelerated version of the proximal gradient method is the *fast proximal gradient method*, also known in the literature as *fast iterative shrinkage thresholding algorithm* (FISTA) [30], [31]. When  $G \equiv 0$ , the problem is smooth, and FISTA coincides with Nesterov's optimal gradient method [32]. In this paper we implement a monotone version of FISTA (MFISTA) [19], which guarantees the objective function value is non-increasing with respect to iteration number.

---

### Monotone FISTA Method (MFISTA) For Solving (6)

---

**Input:** An upper bound  $L \geq L_{\nabla F}$ .

**Step 0.** Take  $\mathbf{y}_1 = \mathbf{x}_0, t_1 = 1$ .

**Step k.** ( $k \geq 1$ ) Compute

$$\begin{aligned} \mathbf{z}_k &= \text{prox}_{\frac{1}{L}G} \left( \mathbf{y}_k - \frac{1}{L} \nabla F(\mathbf{y}_k) \right). \\ t_{k+1} &= \frac{1 + \sqrt{1 + 4t_k^2}}{2}. \\ \mathbf{x}_k &= \text{argmin} \{ F(\mathbf{x}) + G(\mathbf{x}) : \mathbf{x} = \mathbf{z}_k, \mathbf{x}_{k-1} \}. \\ \mathbf{y}_{k+1} &= \mathbf{x}_k + \frac{t_k}{t_{k+1}} (\mathbf{z}_k - \mathbf{x}_k) + \frac{t_k - 1}{t_{k+1}} (\mathbf{x}_k - \mathbf{x}_{k-1}). \end{aligned}$$


---

The rate of convergence of the sequence generated by MFISTA is  $O(1/k^2)$ .

**Theorem II.1.** [19] Let  $\{\mathbf{x}_k\}_{k \geq 0}$  be the sequence generated by MFISTA, and let  $\mathbf{x}^*$  be an optimal solution of (6).

Then

$$F(\mathbf{x}_k) + G(\mathbf{x}_k) - F(\mathbf{x}^*) - G(\mathbf{x}^*) \leq \frac{2L_{\nabla F} \|\mathbf{x}_0 - \mathbf{x}^*\|_2^2}{(k+1)^2}.$$

#### B. The General Nonsmooth Model

The optimization model we consider in this paper is

$$(P) \quad \min_{\mathbf{x} \in \mathbb{R}^n} \{ H(\mathbf{x}) = f(\mathbf{x}) + g(\mathbf{D}^* \mathbf{x}) \},$$

where  $f : \mathbb{R}^n \rightarrow \mathbb{R}$  is a continuously differentiable convex function with a Lipschitz continuous gradient  $L_{\nabla f}$ :

$$\|\nabla f(\mathbf{x}) - \nabla f(\mathbf{y})\|_2 \leq L_{\nabla f} \|\mathbf{x} - \mathbf{y}\|_2 \text{ for all } \mathbf{x}, \mathbf{y} \in \mathbb{R}^n.$$

The function  $g : \mathbb{R}^p \rightarrow \mathbb{R} \cup \{\infty\}$  is a closed, proper convex function which is not necessarily smooth, and  $\mathbf{D}^* \in \mathbb{R}^{p \times n}$  is a given matrix. In addition, we assume that  $g$  is Lipschitz continuous with parameter  $L_g$ :

$$|g(\mathbf{z}) - g(\mathbf{v})| \leq L_g \|\mathbf{z} - \mathbf{v}\|_2 \quad \text{for all } \mathbf{z}, \mathbf{v} \in \mathbb{R}^p.$$

This is equivalent to saying that the subgradients of  $g$  over  $\mathbb{R}^p$  are bounded by  $L_g$ :

$$\|g'(\mathbf{z})\|_2 \leq L_g \text{ for any } \mathbf{x} \in \mathbb{R}^n \text{ and } g'(\mathbf{z}) \in \partial g(\mathbf{z}).$$

An additional assumption is that the proximal operator of  $\alpha g(\mathbf{z})$  for any  $\alpha > 0$  can be easily computed.

Note that directly applying MFISTA to (P) requires computing the proximal operator of  $g(\mathbf{D}^* \mathbf{x})$ . Despite the fact that we assume that it is easy to compute the proximal operator of  $g(\mathbf{z})$ , it is in general difficult to compute that of  $\alpha g(\mathbf{D}^* \mathbf{x})$ . Therefore we need to transform the problem before utilizing MFISTA, in order to avoid this computation.

When considering ALASSO,  $f(\mathbf{x}) = \frac{1}{2} \|\mathbf{A}\mathbf{x} - \mathbf{b}\|_2^2$  and  $g(\mathbf{D}^* \mathbf{x}) = \lambda \|\mathbf{D}^* \mathbf{x}\|_1$ . The Lipschitz constants are given by  $L_{\nabla f} = \|\mathbf{A}\|_2^2$  and  $L_g = \lambda \sqrt{p}$ . The proximal operator of  $\alpha g(\mathbf{z}) = \alpha \lambda \|\mathbf{z}\|_1$  can be computed as

$$\begin{aligned} \text{prox}_{\alpha g}(\mathbf{z}) &= \arg \min_{\mathbf{v} \in \mathbb{R}^p} \left\{ \alpha \lambda \|\mathbf{z}\|_1 + \frac{1}{2} \|\mathbf{v} - \mathbf{z}\|_2^2 \right\} \\ &= \llbracket \mathbf{z} \rrbracket - \lambda \alpha \text{sgn}(\mathbf{z}), \end{aligned} \tag{7}$$

where  $\llbracket \mathbf{z} \rrbracket_+$  denotes the vector whose components are given by the maximum between  $z_i$  and 0. For brevity, we denote the soft shrinkage operator by

$$\Gamma_{\lambda \alpha}(\mathbf{z}) = \llbracket \mathbf{z} \rrbracket - \lambda \alpha \text{sgn}(\mathbf{z}). \tag{8}$$

Note, however, that there is no explicit expression for the proximal operator of  $g(\mathbf{D}^* \mathbf{x}) = \lambda \|\mathbf{D}^* \mathbf{x}\|_1$ , i.e., there is no closed form solution to

$$\arg \min_{\mathbf{u} \in \mathbb{R}^n} \left\{ \alpha \lambda \|\mathbf{D}^* \mathbf{x}\|_1 + \frac{1}{2} \|\mathbf{u} - \mathbf{x}\|_2^2 \right\}.$$

In the next subsection, we introduce two popular approaches for transforming the problem (P): smoothing and decomposition. We will show in Sections II-D and II-E that both transformations lead to algorithms which only require computation of the proximal operator of  $g(\mathbf{z})$ , and not that of  $g(\mathbf{D}^* \mathbf{x})$ .

### C. The Smoothing and Decomposition Transformations

The first approach to transforming the problem is the smoothing method in which the nonsmooth function  $g(\mathbf{z})$  is replaced by its Moreau envelope  $g_\mu(\mathbf{z})$  which can be seen as a smooth approximation. By letting  $\mathbf{z} = \mathbf{D}^* \mathbf{x}$ , the smoothed problem becomes

$$(\text{P}_\mu) \quad \min_{\mathbf{x} \in \mathbb{R}^n} \{H_\mu(\mathbf{x}) = f(\mathbf{x}) + g_\mu(\mathbf{D}^* \mathbf{x})\}.$$

From the general properties of the Moreau envelope, and from the fact that the norms of the subgradients of  $g$  are bounded above by  $L_g$ , we can deduce and summarize several basic properties of  $g_\mu$  (see [20], [22]):

- $g_\mu$  is continuously differentiable with a Lipschitz constant  $\frac{1}{\mu}$ :

$$\|\nabla g_\mu(\mathbf{z}) - \nabla g_\mu(\mathbf{v})\|_2 \leq \frac{1}{\mu} \|\mathbf{z} - \mathbf{v}\|_2 \text{ for all } \mathbf{z}, \mathbf{v} \in \mathbb{R}^p,$$

- There exists some  $\beta_1, \beta_2 > 0$  such that  $\beta_1 + \beta_2 = L_g$  and  $g(\mathbf{z}) - \beta_1\mu \leq g_\mu(\mathbf{z}) \leq g(\mathbf{z}) + \beta_2\mu$  for all  $\mathbf{z} \in \mathbb{R}^p$ .

The second approach for transforming the problem is the decomposition method in which we consider:

$$(P_\rho) \min_{\mathbf{x} \in \mathbb{R}^n, \mathbf{z} \in \mathbb{R}^p} \left\{ G_\rho(\mathbf{x}, \mathbf{z}) = f(\mathbf{x}) + g(\mathbf{z}) + \frac{\rho}{2} \|\mathbf{z} - \mathbf{D}^* \mathbf{x}\|_2^2 \right\}.$$

This problem can be seen as a penalized version of the following constrained formulation of the original problem (P):

$$\begin{aligned} \min \quad & \{f(\mathbf{x}) + g(\mathbf{z})\} \\ \text{s.t.} \quad & \mathbf{z} = \mathbf{D}^* \mathbf{x}, \\ & \mathbf{x} \in \mathbb{R}^n, \mathbf{z} \in \mathbb{R}^p. \end{aligned}$$

Evidently, there is a close relationship between the approximate models  $(P_\mu)$  and  $(P_\rho)$ . Indeed, fixing  $\mathbf{x}$  and minimizing the objective function of  $(P_\rho)$  with respect to  $\mathbf{z}$  we obtain

$$\begin{aligned} \min_{\mathbf{x} \in \mathbb{R}^n, \mathbf{z} \in \mathbb{R}^p} \left\{ f(\mathbf{x}) + g(\mathbf{z}) + \frac{\rho}{2} \|\mathbf{z} - \mathbf{D}^* \mathbf{x}\|_2^2 \right\} \\ = \min_{\mathbf{x} \in \mathbb{R}^n} \left\{ f(\mathbf{x}) + g_{\frac{1}{\rho}}(\mathbf{D}^* \mathbf{x}) \right\}. \end{aligned}$$

Therefore, the two models are equivalent in the sense that their optimal solution set (limited to  $\mathbf{x}$ ) is the same when  $\mu = \frac{1}{\rho}$ . For analysis sparse recovery, both transformations lead to RALASSO. However, as we shall see, the arising smoothing-based and decomposition-based algorithms and their analysis is very different.

#### D. The Smoothing-Based Method

Since  $(P_\mu)$  is a smooth problem we can apply an optimal first-order method such as MFISTA with  $F = H_\mu = f(\mathbf{x}) + g_\mu(\mathbf{D}^* \mathbf{x})$  and  $G \equiv 0$  in equation (6). The Lipschitz constant of  $H_\mu$  is given by  $L_{\nabla f} + \frac{\|\mathbf{D}\|_2^2}{\mu}$ , and according to (5) the gradient of  $\nabla g_\mu(\mathbf{D}^* \mathbf{x})$  is equal to  $\frac{1}{\mu} \mathbf{D}(\mathbf{D}^* \mathbf{x} - \text{prox}_{\mu g}(\mathbf{D}^* \mathbf{x}))$ . The expression  $\text{prox}_{\mu g}(\mathbf{D}^* \mathbf{x})$  is calculated by first computing  $\text{prox}_{\mu g}(\mathbf{z})$ , and then letting  $\mathbf{z} = \mathbf{D}^* \mathbf{x}$ .

Returning to the analysis sparse recovery problem, after smoothing we obtain the smooth problem

$$\min_{\mathbf{x} \in \mathbb{R}^n} \left\{ H_\mu(\mathbf{x}) = \frac{1}{2} \|\mathbf{A} \mathbf{x} - \mathbf{b}\|_2^2 + g_\mu(\mathbf{D}^* \mathbf{x}) \right\}, \quad (9)$$

where

$$\begin{aligned} g_\mu(\mathbf{D}^* \mathbf{x}) &= \min_{\mathbf{u}} \left\{ \lambda \|\mathbf{u}\|_1 + \frac{1}{2\mu} \|\mathbf{u} - \mathbf{D}^* \mathbf{x}\|_2^2 \right\} \\ &= \sum_{i=1}^p \lambda \mathcal{H}_{\lambda\mu}((\mathbf{D}^* \mathbf{x})[i]). \end{aligned}$$



The function  $\mathcal{H}_\alpha(x)$  with parameter  $\alpha > 0$  is the so-called the Huber function [33], and is given by

$$\mathcal{H}_\alpha(x) = \begin{cases} \frac{1}{2\alpha}x^2 & \text{if } |x| < \alpha \\ |x| - \frac{\alpha}{2} & \text{otherwise.} \end{cases}$$

From (7), the gradient of  $g_\mu(\mathbf{D}^*\mathbf{x})$  is equal to

$$\nabla g_\mu(\mathbf{D}^*\mathbf{x}) = \frac{1}{\mu}\mathbf{D}(\mathbf{D}^*\mathbf{x} - \Gamma_{\lambda\mu}(\mathbf{D}^*\mathbf{x})),$$

where  $\Gamma_{\lambda\mu}$  is given by (8). Applying MFISTA to (9), results in the SFISTA algorithm, summarized in Algorithm 1.

---

**Algorithm1: Smoothing-based MFISTA (SFISTA)**

---

**Input:** An upper bound  $L \geq \|\mathbf{A}\|_2^2 + \frac{\|\mathbf{D}\|_2^2}{\mu}$ .

**Step 0.** Take  $\mathbf{y}_1 = \mathbf{x}_0, t_1 = 1$ .

**Step k.** ( $k \geq 1$ ) Compute

$$\nabla f(\mathbf{y}_k) = \mathbf{A}^*(\mathbf{A}\mathbf{y}_k - \mathbf{b}).$$

$$\mathbf{z}_k = \mathbf{y}_k - \frac{1}{L}(\nabla f(\mathbf{y}_k) + \frac{1}{\mu}\mathbf{D}(\mathbf{D}^*\mathbf{x} - \Gamma_{\lambda\mu}(\mathbf{D}^*\mathbf{x}))).$$

$$t_{k+1} = \frac{1 + \sqrt{1 + 4t_k^2}}{2}.$$

$$\mathbf{x}_k = \operatorname{argmin}\{H_\mu(\mathbf{x}) : \mathbf{x} = \mathbf{z}_k, \mathbf{x}_{k-1}\}.$$

$$\mathbf{y}_{k+1} = \mathbf{x}_k + \frac{t_k}{t_{k+1}}(\mathbf{z}_k - \mathbf{x}_k) + \frac{t_k - 1}{t_{k+1}}(\mathbf{x}_k - \mathbf{x}_{k-1}).$$


---

### E. The Decomposition-Based Method

We can also employ MFISTA on the decomposition model

$$\min_{\mathbf{x} \in \mathbb{R}^n, \mathbf{z} \in \mathbb{R}^p} \{G_\rho(\mathbf{x}, \mathbf{z}) = F_\rho(\mathbf{x}, \mathbf{z}) + G(\mathbf{x}, \mathbf{z})\},$$

where we take the smooth part as  $F_\rho(\mathbf{x}, \mathbf{z}) = f(\mathbf{x}) + \frac{\rho}{2}\|\mathbf{z} - \mathbf{D}^*\mathbf{x}\|_2^2$  and the nonsmooth part as  $G(\mathbf{x}, \mathbf{z}) = g(\mathbf{z})$ .

In order to apply MFISTA to (P<sub>ρ</sub>), we need to compute the proximal operator of  $\alpha G$  for a given constant  $\alpha > 0$ , which is given by

$$\begin{aligned} & \operatorname{prox}_{\alpha G}(\mathbf{x}, \mathbf{z}) \\ &= \operatorname{argmin}_{\mathbf{u} \in \mathbb{R}^n, \mathbf{v} \in \mathbb{R}^p} \left\{ \frac{1}{2}\|\mathbf{u} - \mathbf{x}\|^2 + \frac{1}{2}\|\mathbf{v} - \mathbf{z}\|^2 + \alpha g(\mathbf{v}) \right\} \\ &= \begin{pmatrix} \mathbf{x} \\ \operatorname{prox}_{\alpha g}(\mathbf{z}) \end{pmatrix}. \end{aligned}$$

In RALASSO,  $G(\mathbf{x}, \mathbf{z}) = \lambda \|\mathbf{z}\|_1$  and  $F_\rho(\mathbf{x}, \mathbf{z}) = \frac{1}{2} \|\mathbf{A}\mathbf{x} - \mathbf{b}\|_2^2 + \frac{1}{2} \rho \|\mathbf{z} - \mathbf{D}^* \mathbf{x}\|_2^2$ . Therefore,

$$\text{prox}_{\alpha G}(\mathbf{x}, \mathbf{z}) = \begin{pmatrix} \mathbf{x} \\ \Gamma_{\lambda\alpha}(\mathbf{z}) \end{pmatrix}.$$

The Lipschitz constant of  $\nabla F$  is equal to  $(\|\mathbf{A}\|_2^2 + \rho(1 + \|\mathbf{D}\|_2^2))$ . By applying MFISTA directly to RALASSO, we have the DFISTA algorithm, stated in Algorithm 2.

### Algorithm 2: Decomposition-based MFISTA (DFISTA)

**Input:** An upper bound  $L \geq (\|\mathbf{A}\|_2^2 + \rho(1 + \|\mathbf{D}\|_2^2))$ .

**Step 0.** Take  $\mathbf{u}_1 = \mathbf{x}_0, \mathbf{v}_1 = \mathbf{z}_0, t_1 = 1$ .

**Step k.** ( $k \geq 1$ ) Compute

$$\nabla_{\mathbf{x}} F_\rho(\mathbf{u}_k, \mathbf{v}_k) = \mathbf{A}^*(\mathbf{A}\mathbf{u}_k - \mathbf{b}) + \rho \mathbf{D}(\mathbf{D}^* \mathbf{u}_k - \mathbf{v}_k).$$

$$\nabla_{\mathbf{z}} F_\rho(\mathbf{u}_k, \mathbf{v}_k) = \rho(\mathbf{v}_k - \mathbf{D}^* \mathbf{u}_k).$$

$$\mathbf{p}_k = \mathbf{u}_k - \frac{1}{L} \nabla_{\mathbf{x}} F(\mathbf{u}_k, \mathbf{v}_k).$$

$$\mathbf{q}_k = \Gamma_{\frac{\rho}{L}}(\mathbf{v}_k - \frac{1}{L} \nabla_{\mathbf{z}} F(\mathbf{u}_k, \mathbf{v}_k)).$$

$$t_{k+1} = \frac{1 + \sqrt{1 + 4t_k^2}}{2}.$$

$$(\mathbf{x}_k, \mathbf{z}_k)$$

$$= \text{argmin}\{G_\rho(\mathbf{x}, \mathbf{z}) : (\mathbf{x}, \mathbf{z}) = (\mathbf{p}_k, \mathbf{q}_k), (\mathbf{x}_{k-1}, \mathbf{z}_{k-1})\}.$$

$$\mathbf{u}_{k+1} = \mathbf{x}_k + \frac{t_k}{t_{k+1}}(\mathbf{p}_k - \mathbf{x}_k) + \frac{t_k - 1}{t_{k+1}}(\mathbf{x}_k - \mathbf{x}_{k-1}).$$

$$\mathbf{v}_{k+1} = \mathbf{z}_k + \frac{t_k}{t_{k+1}}(\mathbf{q}_k - \mathbf{z}_k) + \frac{t_k - 1}{t_{k+1}}(\mathbf{z}_k - \mathbf{z}_{k-1}).$$

### III. CONVERGENCE ANALYSIS

In this section we analyze the convergence behavior of both the smoothing-based and decomposition-based methods. Convergence of smoothing algorithms has been treated in [22], [20]. In order to make the paper self contained, we quote the main results here. We then analyze the convergence of the decomposition approach. Both methods require the same type of operations at each iteration: the computation of the gradient of the smooth function  $f$ , and of the proximal operator corresponding to  $\alpha g$ , which means that they have the same computational cost per iteration. However, we show that smoothing converges faster than decomposition based methods. Specifically, the smoothing-based algorithm is guaranteed to generate an  $\varepsilon$ -optimal solution within  $O(1/\varepsilon)$  iterations, whereas the decomposition-based approach requires  $O(1/\varepsilon^{1.5})$  iterations. We prove the results by analyzing SFISTA and DFISTA for the general problem (P), however, the same analysis can be easily extended to other optimal first-order methods, such as the one described in [22].

### A. Convergence of the Smoothing-Based Method

For SFISTA the sequence  $\{\mathbf{x}_k\}$  satisfies the following relationship [19]:

$$H_\mu(\mathbf{x}_k) - H_\mu(\mathbf{x}_\mu^*) \leq \frac{2 \left( L_{\nabla f} + \frac{\|\mathbf{D}\|_2^2}{\mu} \right) \Lambda_1}{(k+1)^2}, \quad (10)$$

where  $\Lambda_1$  is an upper bound on the expression  $\|\mathbf{x}_\mu^* - \mathbf{x}_0\|_2$  with  $\mathbf{x}_\mu^*$  being an arbitrary optimal solution of the smoothed problem  $(P_\mu)$ , and  $\mathbf{x}_0$  is the initial point of the algorithm. Of course, this rate of convergence is problematic since we are more interested in bounding the expression  $H(\mathbf{x}_k) - H^*$  rather than the expression  $H_\mu(\mathbf{x}_k) - H_\mu(\mathbf{x}_\mu^*)$ , which is in terms of the smoothed problem. For that, we can use the following result from [20].

**Theorem III.1.** [20] *Let  $\{\mathbf{x}_k\}$  be the sequence generated by applying MFISTA to the problem  $(P_\mu)$ . Let  $\mathbf{x}_0$  be the initial point and let  $\mathbf{x}^*$  denote the optimal solution of  $(P)$ . An  $\varepsilon$ -optimal solution of  $(P)$ , i.e.  $|H(\mathbf{x}_k) - H(\mathbf{x}^*)| \leq \varepsilon$ , is obtained in the smoothing-based method using MFISTA after at most*

$$K = 2\|\mathbf{D}\|_2\sqrt{L_g}\Lambda_1\frac{1}{\varepsilon} + \sqrt{L_{\nabla f}\Lambda_1}\frac{1}{\sqrt{\varepsilon}}$$

iterations with  $\mu$  chosen as

$$\mu = \sqrt{\frac{\|\mathbf{D}\|_2^2}{L_g} \frac{\varepsilon}{\sqrt{\|\mathbf{D}\|_2^2 L_g} + \sqrt{\|\mathbf{D}\|_2^2 L_g + L_{\nabla f} \varepsilon}}},$$

in which  $L_g$  and  $L_{\nabla f}$  are the Lipschitz constants of  $g$  and the gradient function of  $f$  in  $(P)$ , and  $\Lambda_1 = \|\mathbf{x}_0 - \mathbf{x}_\mu^*\|_2$ . We use  $\mathbf{x}_\mu^*$  to denote the optimal solution of problem  $(P_\mu)$ .

**Remarks:** For analysis sparse recovery using SFISTA,  $L_g = \lambda p^{\frac{1}{2}}$  and  $L_{\nabla f} = \|\mathbf{A}\|_2^2$ , which can be plugged into the expressions in the theorem.

### B. Convergence of the Decomposition-Based Method

A key property of the decomposition model  $(P_\rho)$  is that its minimal value is bounded above by the optimal value  $H^*$  in the original problem  $(P)$ .

**Lemma III.1.** *Let  $G_\rho^*$  be the optimal value of problem  $(P_\rho)$  and  $H^*$  be the optimal value of problem  $(P)$ . Then  $G_\rho^* \leq H^*$ .*

**Proof:** The proof follows from adding the constraint  $\mathbf{z} = \mathbf{D}^* \mathbf{x}$  to the optimization:

$$\begin{aligned} G_\rho^* &= \min_{\mathbf{x} \in \mathbb{R}^n, \mathbf{z} \in \mathbb{R}^p} \left\{ f(\mathbf{x}) + g(\mathbf{z}) + \frac{\rho}{2} \|\mathbf{z} - \mathbf{D}^* \mathbf{x}\|_2^2 \right\} \\ &\leq \min_{\mathbf{x} \in \mathbb{R}^n, \mathbf{z} \in \mathbb{R}^p, \mathbf{z} = \mathbf{D}^* \mathbf{x}} \left\{ f(\mathbf{x}) + g(\mathbf{z}) + \frac{\rho}{2} \|\mathbf{z} - \mathbf{D}^* \mathbf{x}\|_2^2 \right\} \\ &= \min_{\mathbf{x} \in \mathbb{R}^n} \{ f(\mathbf{x}) + g(\mathbf{D}^* \mathbf{x}) \}, \end{aligned}$$

which is equal to  $H^*$ .

The next theorem is our main convergence result establishing that an  $\varepsilon$ -optimal solution can be reached after  $O(1/\varepsilon^{1.5})$  iterations. By assuming that the functions  $f$  and  $g$  are nonnegative, which is not an unusual assumption, we have the following theorem.

**Theorem III.2.** *Let  $\{\mathbf{x}_k, \mathbf{z}_k\}$  be the sequences generated by applying MFISTA to  $(P_\rho)$ . The initial point is taken as  $(\mathbf{x}_0, \mathbf{z}_0)$  with  $\mathbf{z}_0 = \mathbf{D}^* \mathbf{x}_0$ . Let  $\mathbf{x}^*$  denote the optimal solution of the original problem (P). An  $\varepsilon$ -optimal solution of problem (P), i.e.  $|H(\mathbf{x}_k) - H(\mathbf{x}^*)| \leq \varepsilon$ , is obtained using the decomposition-based method after at most*

$$K = \max \left\{ \frac{16\sqrt{(1 + \|\mathbf{D}\|^2 \Lambda_2 H(\mathbf{x}_0))} L_g}{\varepsilon^{1.5}}, \frac{2\sqrt{L_{\nabla f} \Lambda_2}}{\sqrt{\varepsilon}} \right\}$$

iterations of MFISTA with  $\rho$  chosen as

$$\rho = \left( \frac{L_g \sqrt{2H(\mathbf{x}_0)} K^2}{2(1 + \|\mathbf{D}\|^2) \Lambda_2} \right)^{2/3}.$$

Here  $L_g$  and  $L_{\nabla f}$  are the Lipschitz constants for  $g$  and the gradient function of  $f$  in (P), and  $\Lambda_2 = \|\mathbf{x}_0 - \mathbf{x}_\rho^*\|_2^2 + \|\mathbf{z}_0 - \mathbf{z}_\rho^*\|_2^2$ . We use  $\mathbf{x}_\rho^*, \mathbf{z}_\rho^*$  to denote the optimal solutions of problem  $(P_\rho)$ .

**Proof:** Since the monotone version of FISTA is applied we have

$$\begin{aligned} f(\mathbf{x}_k) + g(\mathbf{z}_k) + \frac{\rho}{2} \|\mathbf{z}_k - \mathbf{D}^* \mathbf{x}_k\|_2^2 \\ = G_\rho(\mathbf{x}_k, \mathbf{z}_k) \leq G_\rho(\mathbf{x}_0, \mathbf{z}_0) = f(\mathbf{x}_0) + g(\mathbf{D}^* \mathbf{x}_0) = H(\mathbf{x}_0). \end{aligned} \quad (11)$$

With the assumption that  $f$  and  $g$  are nonnegative, it follows that

$$\frac{\rho}{2} \|\mathbf{z}_k - \mathbf{D}^* \mathbf{x}_k\|_2^2 \leq H(\mathbf{x}_0),$$

and therefore

$$\|\mathbf{z}_k - \mathbf{D}^* \mathbf{x}_k\|_2 \leq \sqrt{\frac{2H(\mathbf{x}_0)}{\rho}}. \quad (12)$$

The gradient of  $f(\mathbf{x}) + \frac{\rho}{2} \|\mathbf{z} - \mathbf{D}^* \mathbf{x}\|_2^2$ , is Lipschitz continuous with parameter  $(L_{\nabla f} + \rho(1 + \|\mathbf{D}\|_2^2))$ . According to [19], by applying MFISTA, we obtain a sequence  $\{(\mathbf{x}_k, \mathbf{z}_k)\}$  satisfying

$$G_\rho(\mathbf{x}_k, \mathbf{z}_k) - G_\rho^* \leq \frac{2(L_{\nabla f} + \rho(1 + \|\mathbf{D}\|_2^2)) \Lambda_2}{k^2}.$$

Using lemma III.1 and the notation

$$A = 2L_{\nabla f} \Lambda_2, \text{ and } B = 2(1 + \|\mathbf{D}\|_2^2) \Lambda_2,$$

we have

$$G_\rho(\mathbf{x}_k, \mathbf{z}_k) - H^* \leq \frac{A + \rho B}{k^2}. \quad (13)$$

We therefore conclude that

$$\begin{aligned}
H(\mathbf{x}_k) &= f(\mathbf{x}_k) + g(\mathbf{D}^* \mathbf{x}_k) \\
&= f(\mathbf{x}_k) + g(\mathbf{z}_k) + g(\mathbf{D}^* \mathbf{x}_k) - g(\mathbf{z}_k) \\
&\leq G_\rho(\mathbf{x}_k, \mathbf{z}_k) + L_g \|\mathbf{z}_k - \mathbf{D}^* \mathbf{x}_k\|_2 \\
&\leq H^* + \frac{A + \rho B}{k^2} + L_g \|\mathbf{z}_k - \mathbf{D}^* \mathbf{x}_k\|_2 \\
&\leq H^* + \frac{A + \rho B}{k^2} + L_g \sqrt{\frac{2H(\mathbf{x}_0)}{\rho}}.
\end{aligned}$$

The first inequality follows from the Lipschitz condition for the function  $g$ , the second inequality is obtained from (13), and the last inequality is a result of (12).

We now seek the “best”  $\rho$  that minimizes the upper bound, or equivalently, minimizes the term

$$\frac{A + \rho B}{k^2} + L_g \sqrt{\frac{2H(\mathbf{x}_0)}{\rho}} = C\rho + \frac{D}{\sqrt{\rho}},$$

where  $C = \frac{B}{k^2}$  and  $D = L_g \sqrt{2H(\mathbf{x}_0)}$ . Setting the derivative to zero, the optimal value of  $\rho$  is  $\rho = \left(\frac{D}{2C}\right)^{2/3}$ , and

$$H(\mathbf{x}_k) \leq H^* + \frac{A}{k^2} + 2C^{1/3} D^{2/3}.$$

Therefore, to obtain an  $\varepsilon$ -optimal solution, it is enough that

$$\frac{A}{k^2} \leq \frac{\varepsilon}{2}, \quad \frac{2B^{1/3} D^{2/3}}{k^{2/3}} \leq \frac{\varepsilon}{2},$$

or

$$\begin{aligned}
k &\geq \max \left\{ \frac{4^{3/2} B^{1/2} D}{\varepsilon^{1.5}}, \frac{\sqrt{2A}}{\sqrt{\varepsilon}} \right\} \\
&= \max \left\{ \frac{16\sqrt{(1 + \|\mathbf{D}\|^2 \Lambda_2 H(\mathbf{x}_0))} L_g}{\varepsilon^{1.5}}, \frac{2\sqrt{L_{\nabla f} \Lambda_2}}{\sqrt{\varepsilon}} \right\},
\end{aligned}$$

completing the proof.

**Remarks:** As in SFISTA, when treating the analysis sparse recovery problem,  $L_g = \lambda p^{\frac{1}{2}}$  and  $L_{\nabla f} = \|\mathbf{A}\|_2^2$ , which again can be plugged into the expressions in the theorem.

Comparing the results of smoothing-based and decomposition-based methods, we immediately conclude that the smoothing-based method is preferable. First, it requires only  $O(1/\varepsilon)$  iterations to obtain an  $\varepsilon$ -optimal solution whereas the decomposition approach necessitates  $O(1/\varepsilon^{3/2})$  iterations. Note, that both bounds are better than the bound  $O(1/\varepsilon^2)$  corresponding to general sub-gradient schemes for nonsmooth optimization. Second, the bound in the smoothing approach depends on  $\sqrt{L_g}$ , and not on  $L_g$ , as when using decomposition methods. This is important since, for example, when  $g(\mathbf{z}) = \|\mathbf{z}\|_1$ , we have  $L_g = p^{\frac{1}{2}}$ . In the smoothing approach the dependency on  $p$  is of the form  $p^{\frac{1}{4}}$  and not  $p^{\frac{1}{2}}$ , as when using the decomposition algorithm.

#### IV. PERFORMANCE BOUNDS

We now turn to analyze the recovery performance of analysis LASSO when smoothing and decomposition are applied. As we have seen, both transformations lead to the same relaxed ALASSO problem:

$$(\text{RALASSO}) \min_{\mathbf{x} \in \mathbb{R}^n, \mathbf{z} \in \mathbb{R}^p} \frac{1}{2} \|\mathbf{A}\mathbf{x} - \mathbf{b}\|_2^2 + \lambda \|\mathbf{z}\|_1 + \frac{1}{2} \rho \|\mathbf{z} - \mathbf{D}^* \mathbf{x}\|_2^2,$$

in which  $\mathbf{A} \in \mathbb{R}^{m \times n}$ ,  $\mathbf{D} \in \mathbb{R}^{n \times p}$ ,  $\mathbf{x} \in \mathbb{R}^n$  and  $\mathbf{z} \in \mathbb{R}^p$ . Our main result in this section shows that the reconstruction obtained by solving RALASSO is stable when  $\mathbf{D}^* \mathbf{x}$  has rapidly decreasing coefficients and the noise in the model (M) is small enough. Our performance bound also depends on the choice of parameter  $\rho$  in the objective function. Before stating the main theorems, we first introduce a definition and some useful lemmas, whose proofs are detailed in the Appendix.

To ensure stable recovery, we require that the matrix  $\mathbf{A}$  satisfies the D-RIP:

**Definition IV.1.** (*D-RIP*) [12]. *The measurement matrix  $\mathbf{A}$  obeys the restricted isometry property adapted to  $\mathbf{D}$  with constant  $\sigma_s$  if*

$$(1 - \sigma_s) \|\mathbf{v}\|_2^2 \leq \|\mathbf{A}\mathbf{v}\|_2^2 \leq (1 + \sigma_s) \|\mathbf{v}\|_2^2$$

*holds for all  $\mathbf{v} \in \Sigma_s = \{\mathbf{y} : \mathbf{y} = \mathbf{D}\mathbf{x} \text{ and } \|\mathbf{x}\|_0 \leq s\}$ . In other words,  $\Sigma_s$  is the union of subspaces spanned by all subsets of  $s$  columns of  $\mathbf{D}$ .*

The following lemma provides a useful inequality for matrices satisfying D-RIP.

**Lemma IV.1.** *Let  $\mathbf{A}$  satisfy the D-RIP with parameter  $\sigma_{2s}$ , and assume that  $\mathbf{u}, \mathbf{v} \in \Sigma_s$ . Then,*

$$\text{Re}\langle \mathbf{A}\mathbf{u}, \mathbf{A}\mathbf{v} \rangle \geq -\sigma_{2s} \|\mathbf{u}\|_2 \|\mathbf{v}\|_2 + \text{Re}\langle \mathbf{u}, \mathbf{v} \rangle.$$

In the following,  $\mathbf{x}_{\text{opt}}$  denotes the optimal solution of RALASSO and  $\mathbf{x}$  as the original signal in the linear model (M); we also use  $\mathbf{h}$  to represent the reconstruction error  $\mathbf{h} = \mathbf{x}_{\text{opt}} - \mathbf{x}$ . Let  $\mathcal{T}$  be the indices of coefficients with  $s$  largest magnitudes in the vector  $\mathbf{D}^* \mathbf{x}$ , and denote the complement of  $\mathcal{T}$  by  $\mathcal{T}^c$ . Setting  $\mathcal{T}_0 = \mathcal{T}$ , we decompose  $\mathcal{T}_0^c$  into sets of size  $s$  where  $\mathcal{T}_1$  denotes the locations of the  $s$  largest coefficients in  $\mathbf{D}_{\mathcal{T}^c}^* \mathbf{x}$ ,  $\mathcal{T}_2$  denote the next  $s$  largest coefficients and so on. Finally, we let  $\mathcal{T}_{01} = \mathcal{T}_0 \cup \mathcal{T}_1$ .

Using the result of Lemma IV.1 and the inequality  $\|\mathbf{D}_{\mathcal{T}_0}^* \mathbf{h}\|_2 + \|\mathbf{D}_{\mathcal{T}_1}^* \mathbf{h}\|_2 \leq \sqrt{2} \|\mathbf{D}_{\mathcal{T}_{01}}^* \mathbf{h}\|_2$  since  $\mathcal{T}_0$  and  $\mathcal{T}_1$  are disjoint, we have the following lemma.

**Lemma IV.2.** (*D-RIP property*) *Let  $\mathbf{h} = \mathbf{x}_{\text{opt}} - \mathbf{x}$  be the reconstruction error in RALASSO. We assume that  $\mathbf{A}$  satisfies the D-RIP with parameter  $\sigma_{2s}$  and  $\mathbf{D}$  is a tight frame. Then,*

$$\begin{aligned} & \text{Re}\langle \mathbf{A}\mathbf{h}, \mathbf{A}\mathbf{D}\mathbf{D}_{\mathcal{T}_{01}}^* \mathbf{h} \rangle \\ & \geq (1 - \sigma_{2s}) \|\mathbf{D}_{\mathcal{T}_{01}}^* \mathbf{h}\|_2^2 - \sqrt{2} s^{-\frac{1}{2}} \sigma_{2s} \|\mathbf{D}_{\mathcal{T}_{01}}^* \mathbf{h}\|_2 \|\mathbf{D}_{\mathcal{T}^c}^* \mathbf{h}\|_1. \end{aligned}$$

Finally, the lemmas below show that the reconstruction error  $\mathbf{h}$  and  $\|\mathbf{D}_{\mathcal{T}^c}^* \mathbf{h}\|_1$  can not be very large.

**Lemma IV.3. (Optimality condition)** The optimal solution  $\mathbf{x}_{\text{opt}}$  for RALASSO satisfies

$$\|\mathbf{D}^* \mathbf{A}^* \mathbf{A} \mathbf{h}\|_{\infty} \leq \left( \frac{1}{2} + \|\mathbf{D}^* \mathbf{D}\|_{1,1} \right) \lambda.$$

**Lemma IV.4. (Cone constraint)** For RALASSO optimization, we have  $\mathbf{D}_{\mathcal{T}^c}^* \mathbf{h}$  obeying the following cone constraint,

$$\|\mathbf{D}_{\mathcal{T}^c}^* \mathbf{h}\|_1 \leq \frac{\lambda}{\rho} p + 3\|\mathbf{D}_{\mathcal{T}}^* \mathbf{h}\|_1 + 4\|\mathbf{D}_{\mathcal{T}^c}^* \mathbf{x}\|_1.$$

We are now ready to state our main result.

**Theorem IV.1.** Let  $\mathbf{A}$  be an  $m \times n$  measurement matrix,  $\mathbf{D}$  an arbitrary  $n \times p$  tight frame, and let  $\mathbf{A}$  satisfy the  $D$ -RIP with  $\sigma_{2s} < 0.1907$ . Consider the measurement  $\mathbf{b} = \mathbf{A} \mathbf{x} + \mathbf{w}$ , where  $\mathbf{w}$  is noise that satisfies  $\|\mathbf{D}^* \mathbf{A}^* \mathbf{w}\|_{\infty} \leq \frac{\lambda}{2}$ . Then the solution  $\mathbf{x}_{\text{opt}}$  to RALASSO satisfies

$$\|\mathbf{x}_{\text{opt}} - \mathbf{x}\|_2 \leq C_0 \sqrt{s} \lambda + C_1 \frac{\|\mathbf{D}^* \mathbf{x} - (\mathbf{D}^* \mathbf{x})_s\|_1}{\sqrt{s}} + C_2 \frac{\lambda p}{\sqrt{s} \rho}, \quad (14)$$

for the decomposition transformation and

$$\|\mathbf{x}_{\text{opt}} - \mathbf{x}\|_2 \leq C_0 \sqrt{s} \lambda + C_1 \frac{\|\mathbf{D}^* \mathbf{x} - (\mathbf{D}^* \mathbf{x})_s\|_1}{\sqrt{s}} + C_2 \frac{\lambda \mu p}{\sqrt{s}}, \quad (15)$$

for the smoothing transformation. Here  $(\mathbf{D}^* \mathbf{x})_s$  is the vector consisting of the largest  $s$  entries of  $\mathbf{D}^* \mathbf{x}$  in magnitude,  $C_1$  and  $C_2$  are constants depending on  $\sigma_{2s}$ , and  $C_0$  depends on  $\sigma_{2s}$  and  $\|\mathbf{D}^* \mathbf{D}\|_{1,1}$ .

**Proof:** The proof follows mainly from the ideas in [9], [26]. The proof proceeds in two steps. First, we try to show that  $\mathbf{D}^* \mathbf{h}$  inside  $\mathcal{T}_{01}$  is bounded by the terms of  $\mathbf{D}^* \mathbf{h}$  outside the set  $\mathcal{T}$ . Then we show that  $\mathbf{D}_{\mathcal{T}^c}^* \mathbf{h}$  is essentially small. From Lemma IV.2,

$$\begin{aligned} & \text{Re} \langle \mathbf{A} \mathbf{h}, \mathbf{A} \mathbf{D} \mathbf{D}_{\mathcal{T}_{01}}^* \mathbf{h} \rangle \\ & \geq (1 - \sigma_{2s}) \|\mathbf{D}_{\mathcal{T}_{01}}^* \mathbf{h}\|_2^2 - \sqrt{2s}^{-\frac{1}{2}} \sigma_{2s} \|\mathbf{D}_{\mathcal{T}_{01}}^* \mathbf{h}\|_2 \|\mathbf{D}_{\mathcal{T}^c}^* \mathbf{h}\|_1. \end{aligned} \quad (16)$$

Using the fact that  $\text{Re} \langle \mathbf{x}, \mathbf{y} \rangle \leq \|\langle \mathbf{x}, \mathbf{y} \rangle\| \leq \|\mathbf{x}\|_1 \|\mathbf{y}\|_{\infty}$ , we obtain that

$$\begin{aligned} \text{Re} \langle \mathbf{A} \mathbf{h}, \mathbf{A} \mathbf{D} \mathbf{D}_{\mathcal{T}_{01}}^* \mathbf{h} \rangle &= \text{Re} \langle \mathbf{D}^* \mathbf{A}^* \mathbf{A} \mathbf{h}, \mathbf{D}_{\mathcal{T}_{01}}^* \mathbf{h} \rangle \\ &\leq \|\mathbf{D}^* \mathbf{A}^* \mathbf{A} \mathbf{h}\|_{\infty} \|\mathbf{D}_{\mathcal{T}_{01}}^* \mathbf{h}\|_1 \\ &\leq \sqrt{2s} c_0 \lambda \|\mathbf{D}_{\mathcal{T}_{01}}^* \mathbf{h}\|_2. \end{aligned} \quad (17)$$

Here we have  $c_0 = \frac{1}{2} + \|\mathbf{D}^* \mathbf{D}\|_{1,1}$ . The second inequality is a result of Lemma IV.3 and the fact that  $\|\mathbf{D}_{\mathcal{T}_{01}}^* \mathbf{h}\|_1 \leq \sqrt{2s} \|\mathbf{D}_{\mathcal{T}_{01}}^* \mathbf{h}\|_2$ , in which  $2s$  is the number of nonzero terms in  $\mathbf{D}_{\mathcal{T}_{01}}^* \mathbf{h}$ . Combining (16) and (17), we get

$$\|\mathbf{D}_{\mathcal{T}_{01}}^* \mathbf{h}\|_2 \leq \frac{\sqrt{2s} \lambda c_0 + \sqrt{2s}^{-\frac{1}{2}} \sigma_{2s} \|\mathbf{D}_{\mathcal{T}^c}^* \mathbf{h}\|_1}{1 - \sigma_{2s}}. \quad (18)$$

Then the second step bounds  $\|\mathbf{D}_{\mathcal{T}^c}^* \mathbf{h}\|_1$ . From (18) we conclude that

$$\begin{aligned} \|\mathbf{D}_{\mathcal{T}}^* \mathbf{h}\|_1 &\leq \sqrt{s} \|\mathbf{D}_{\mathcal{T}}^* \mathbf{h}\|_2 \leq \sqrt{s} \|\mathbf{D}_{\mathcal{T}_{01}}^* \mathbf{h}\|_2 \\ &\leq \frac{\sqrt{2} \lambda s c_0 + \sqrt{2} \sigma_{2s} \|\mathbf{D}_{\mathcal{T}^c}^* \mathbf{h}\|_1}{1 - \sigma_{2s}}. \end{aligned} \quad (19)$$

Finally, using Lemma IV.4 and (19),

$$\|\mathbf{D}_{\mathcal{T}^c}^* \mathbf{h}\|_1 \leq \frac{\lambda}{\rho} p + \frac{3\sqrt{2}\lambda s c_0 + 3\sqrt{2}\sigma_{2s} \|\mathbf{D}_{\mathcal{T}^c}^* \mathbf{h}\|_1}{1 - \sigma_{2s}} + 4\|\mathbf{D}_{\mathcal{T}^c}^* \mathbf{x}\|_1.$$

Since  $\sigma_{2s} < 0.1907$ , we have  $1 - (1 + 3\sqrt{2})\sigma_{2s} > 0$ . Rearranging terms, the above inequality becomes

$$\begin{aligned} & \|\mathbf{D}_{\mathcal{T}^c}^* \mathbf{h}\|_1 \\ & \leq \frac{1 - \sigma_{2s}}{1 - (1 + 3\sqrt{2})\sigma_{2s}} \frac{\lambda}{\rho} p + \frac{3\sqrt{2}\lambda s c_0 + 4(1 - \sigma_{2s})\|\mathbf{D}_{\mathcal{T}^c}^* \mathbf{x}\|_1}{1 - (1 + 3\sqrt{2})\sigma_{2s}}. \end{aligned} \quad (20)$$

We now derive the bound on the reconstruction error. Using the results of (18) and (20), we get

$$\begin{aligned} \|\mathbf{h}\|_2 &= \|\mathbf{D}^* \mathbf{h}\|_2 \leq \|\mathbf{D}_{\mathcal{T}_0}^* \mathbf{h}\|_2 + \sum_{j \geq 2} \|\mathbf{D}_{\mathcal{T}_j}^* \mathbf{h}\|_2 \\ &\leq \frac{\sqrt{2s}\lambda c_0 + \sqrt{2}s^{-\frac{1}{2}}\sigma_{2s} \|\mathbf{D}_{\mathcal{T}^c}^* \mathbf{h}\|_1}{1 - \sigma_{2s}} + s^{-\frac{1}{2}} \|\mathbf{D}_{\mathcal{T}^c}^* \mathbf{h}\|_1 \\ &= \frac{c_0 \lambda \sqrt{2s}}{1 - \sigma_{2s}} + \frac{((\sqrt{2} - 1)\sigma_{2s} + 1)s^{-\frac{1}{2}} \|\mathbf{D}_{\mathcal{T}^c}^* \mathbf{h}\|_1}{1 - \sigma_{2s}} \\ &\leq C_0 \sqrt{s} \lambda + C_1 \frac{\|\mathbf{D}^* \mathbf{x} - (\mathbf{D}^* \mathbf{x})_s\|_1}{\sqrt{s}} + C_2 \frac{\lambda p}{\sqrt{s} \rho}. \end{aligned}$$

The first equality follows from the assumption that  $\mathbf{D}$  is a tight frame and then  $\mathbf{D}\mathbf{D}^* = \mathbf{I}$ . The first inequality uses the triangle inequality. The second inequality follows from  $\sum_{j \geq 2} \|\mathbf{D}_{\mathcal{T}_j}^* \mathbf{h}\|_2 \leq s^{-\frac{1}{2}} \|\mathbf{D}_{\mathcal{T}^c}^* \mathbf{h}\|_1$ , which will be proved in equation 23 in the Appendix. The constants in the final result are given by

$$\begin{aligned} C_0 &= \frac{4\sqrt{2}c_0}{(1 - (1 + 3\sqrt{2})\sigma_{2s})}, \\ C_1 &= \frac{4((\sqrt{2} - 1)\sigma_{2s} + 1)}{1 - (1 + 3\sqrt{2})\sigma_{2s}}, \\ C_2 &= \frac{(\sqrt{2} - 1)\sigma_{2s} + 1}{1 - (1 + 3\sqrt{2})\sigma_{2s}}. \end{aligned}$$

To obtain the error bound for the smoothing transformation we replace  $\rho$  with  $1/\mu$  in the result.  $\square$

Choosing  $\rho \rightarrow \infty$  in RLASSO leads to the ALASSO problem for which  $\mathbf{z} = \mathbf{D}^* \mathbf{x}$ . We then have the following result.

**Theorem IV.2.** *Let  $\mathbf{A}$  be an  $m \times n$  measurement matrix,  $\mathbf{D}$  an arbitrary  $n \times p$  tight frame, and let  $\mathbf{A}$  satisfy the  $D$ -RIP with  $\sigma_{2s} < 0.1907$ . Consider the measurement  $\mathbf{b} = \mathbf{A}\mathbf{x} + \mathbf{w}$ , where  $\mathbf{w}$  is noise that satisfies  $\|\mathbf{D}^* \mathbf{A}^* \mathbf{w}\|_\infty \leq \frac{\lambda}{2}$ . Then the solution  $\mathbf{x}_{\text{opt}}$  to ALASSO satisfies*

$$\|\mathbf{x}_{\text{opt}} - \mathbf{x}\|_2 \leq C_0 \sqrt{s} \lambda + C_1 \frac{\|\mathbf{D}^* \mathbf{x} - (\mathbf{D}^* \mathbf{x})_s\|_1}{\sqrt{s}}, \quad (21)$$

where  $(\mathbf{D}^* \mathbf{x})_s$  is the vector consisting of the largest  $s$  entries of  $\mathbf{D}^* \mathbf{x}$  in magnitude,  $C_1$  is a constant depending on  $\sigma_{2s}$ , and  $C_0$  depends on  $\sigma_{2s}$  and  $\|\mathbf{D}^* \mathbf{D}\|_{1,1}$ .

**Remarks:**



1. When the noise in the system is zero, we can choose  $\lambda = 0$ . The solution  $\mathbf{x}_{\text{opt}}$  then satisfies  $\|\mathbf{x}_{\text{opt}} - \mathbf{x}\| \leq C_1 \frac{\|\mathbf{D}^* \mathbf{x} - (\mathbf{D}^* \mathbf{x})_s\|_1}{\sqrt{s}}$ , which parallels the result for the noiseless synthesis model in [9].

2. When  $\mathbf{D}^*$  is a tight frame, we have  $\mathbf{D}\mathbf{D}^* = \mathbf{I}$ . Therefore by letting  $\mathbf{v} = \mathbf{D}^* \mathbf{x}$ , we can reformulate the original analysis model as

$$\min_{\mathbf{v}} \frac{1}{2} \|\mathbf{A}\mathbf{D}\mathbf{v} - \mathbf{b}\|_2^2 + \lambda \|\mathbf{v}\|_1.$$

Assuming that the noise term satisfies the  $l_2$  norm constraint  $\|\mathbf{w}\|_2 \leq \varepsilon$ , we have  $\|\mathbf{D}^* \mathbf{A}^* \mathbf{w}\|_\infty \leq \|\mathbf{D}^* \mathbf{A}^* \mathbf{w}\|_2 \leq \|\mathbf{D}^* \mathbf{A}^*\|_2 \|\mathbf{w}\|_2 \leq \varepsilon \|\mathbf{D}^* \mathbf{A}^*\|_2$ . When  $\mathbf{A}$  satisfies D-RIP with  $\sigma_{2s} < 0.1907$ , by letting  $\lambda = 2\varepsilon \|\mathbf{D}^* \mathbf{A}^*\|_2$  we have

$$\|\mathbf{v}_{\text{opt}} - \mathbf{v}_0\|_2 \leq \|\mathbf{D}^*\|_2 \|\mathbf{x}_{\text{opt}} - \mathbf{x}\|_2 \leq \tilde{C}_0 \varepsilon + \tilde{C}_1 \frac{\|\mathbf{v}_0 - \mathbf{v}_s\|_1}{\sqrt{s}}. \quad (22)$$

This result has a form similar to the reconstruction error bound shown in [9]. However, the specific constants are different since in [9] the matrix  $\mathbf{A}\mathbf{D}$  is required to satisfy the RIP, whereas in our paper we require only that the D-RIP is satisfied.

3. A similar performance bound is introduced in [26] and shown to be valid when  $\sigma_{3s} < 0.25$ . Using Corollary 3.4 in [27], this is equivalent to  $\sigma_{2s} < 0.0833$ . Thus the results in Theorem IV.2 allow for a looser constraint on ALASSO recovery.

4. The performance bound of Theorem IV.1 implies that a larger choice of  $\rho$ , or a smaller parameter  $\mu$ , leads to a smaller reconstruction error bound. This trend is intuitive since large  $\rho$  or small  $\mu$  results in smaller model inaccuracy. However, a larger  $\rho$  or a smaller  $\mu$  leads to a larger Lipschitz constant and thus results in slower convergence according to Theorem II.1. The idea of parameter continuation [34] can be introduced to both  $\rho$  and  $\mu$  to accelerate the convergence while obtaining a desired reconstruction accuracy. More details will be given in the next section.

## V. NUMERICAL RESULTS

In the numerical examples, we use both randomly generated data and CT image reconstruction to demonstrate that SFISTA performs better than DFISTA. In the last example we also introduce a continuation technique to further speed up convergence of the smoothing-based method.

### A. Randomly Generated Data in a Noiseless Case

In this simulation, the entries in the  $m \times n$  measurement matrix  $\mathbf{A}$  were randomly generated according to a normal distribution. The  $n \times p$  matrix  $\mathbf{D}$  is a random tight frame, where each entry in the matrix is drawn independently from a Gaussian distribution. In the simulation we let  $n = 120$  and  $p = 144$ , and we also set the values of  $m$  and the number of zero terms named  $l$  in  $\mathbf{D}^* \mathbf{x}$  according to the following formula:

$$m = \alpha n, \quad l = n - \beta m.$$

We varied  $\alpha$  and  $\beta$  from 0.1 to 1, with a step size 0.05. We set  $\lambda = 0.004$ ,  $\mu = 10^{-3} \lambda^{-1}$  for the smoothing-based method, and  $\rho = 10^3 \lambda$  for the decomposition-based method. For every combination of  $\alpha$  and  $\beta$ , we ran a Monte

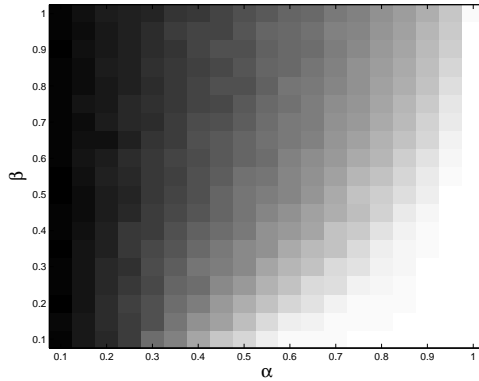


Fig. 1: Reconstruction error of SFISTA

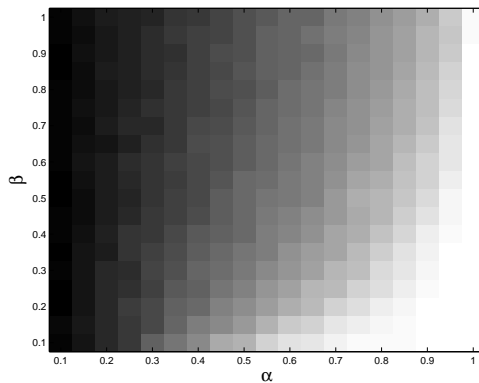


Fig. 2: Reconstruction error of DFISTA

Carlo simulation 50 times. Each algorithm ran for 3000 iterations, and we then took the average reconstruction error. The reconstruction error is defined by  $\frac{\|\mathbf{x}_{\text{opt}} - \mathbf{x}\|}{\|\mathbf{x}\|}$ , in which  $\mathbf{x}_{\text{opt}}$  is the reconstructed signal using smoothing or decomposition and  $\mathbf{x}$  is the original signal in (M).

The average reconstruction error for soothing and decomposition are plotted in Figs. 1 and 2, respectively. White pixels present low reconstruction error whereas black pixels mean high error. Evidently, see that with same number of iterations, SFISTA results in a better reconstruction than DFISTA.

### B. CT Image Reconstruction in a Noisy Case

The next numerical experiment was performed on a noisy  $256 \times 256$  Shepp Logan phantom. The image scale was normalized to  $[0, 1]$ . The additive noise followed a zero-mean Gaussian distribution with standard deviation  $\sigma = 0.001$ . Due to the high cost of projection in CT, we only observed a limited number of radial lines of the phantom's 2D discrete Fourier transform. The matrix  $D^*$  consists of all vertical and horizontal gradients, which leads to a sparse  $D^*\mathbf{x}$ . We let  $\lambda = 0.001$  in the optimization. We tested this CT scenario with  $\mu$  values of

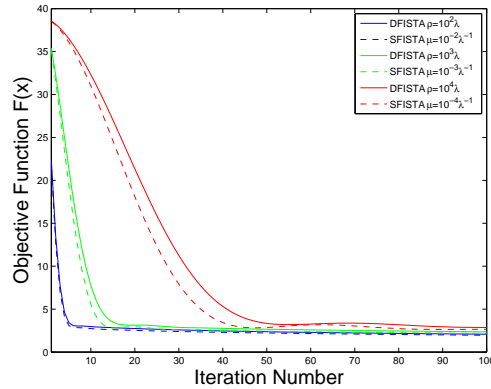


Fig. 3: The objective function for CT reconstruction on Shepp Logan.

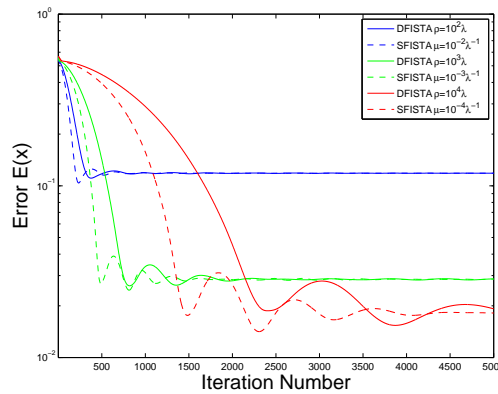


Fig. 4: Reconstruction error for SFISTA and DFISTA with different parameters.

$10^{-2}\lambda^{-1}$ ,  $10^{-3}\lambda^{-1}$ ,  $10^{-4}\lambda^{-1}$  for SFISTA and  $\rho = 10^2\lambda$ ,  $\rho = 10^3\lambda$ ,  $10^4\lambda$  for DFISTA. We performed 12 radial projections to test these two methods.

In Fig. 3 we plot the objective  $\frac{1}{2}\|A\mathbf{x} - \mathbf{b}\|_2^2 + \lambda\|D^*\mathbf{x}\|_1$  as a function of the iteration number. It can be seen that the objective function of SFISTA decreases more rapidly than DFISTA. Furthermore, with smaller  $\rho$  and larger  $\mu$ , DFISTA and SFISTA converge faster. Then we computed the reconstruction error as  $E(\mathbf{x}) = \frac{\|\mathbf{x} - \mathbf{x}_0\|_2}{\|\mathbf{x}_0\|_2}$ , in which  $\mathbf{x}_0$  is the original image. Here we see that smaller  $\mu$  and larger  $\rho$  lead to a more accurate reconstruction.

### C. Acceleration by Continuation

To accelerate convergence, we consider continuation on the parameter  $\mu$  for SFISTA, or on  $\rho$  for DFISTA. From Theorem IV.1, we see that smaller  $\mu$  results in a smaller reconstruction error. At the same time, smaller  $\mu$  leads to a larger Lipschitz constant  $L_{\nabla F}$  in Theorem II.1, and thus results in slower convergence. The idea of continuation is to solve a sequence of similar problems while using the previous solution as a warm start. Taking the smoothing-

based method as an example, we can run SFISTA with  $\mu_1, \mu_2, \mu_3, \dots, \mu_f$ . The continuation method is given in Algorithm 3. The algorithm for applying continuation on the DFISTA is the same.

---

**Algorithm 3: Continuation with SFISTA**

---

**Input:**  $\mathbf{x}$ , the starting parameter  $\mu = \mu_0$ ,  
the ending parameter  $\mu_f$  and  $\gamma > 1$ .  
**Step 1.** run SFISTA with  $\mu$  and initial point  $\mathbf{x}$ .  
**Step 2.** Get the solution  $\mathbf{x}^*$  and let  $\mathbf{x} = \mathbf{x}^*$ ,  $\mu = \mu/\gamma$ .  
**Until.**  $\mu \leq \mu_f$ .

---

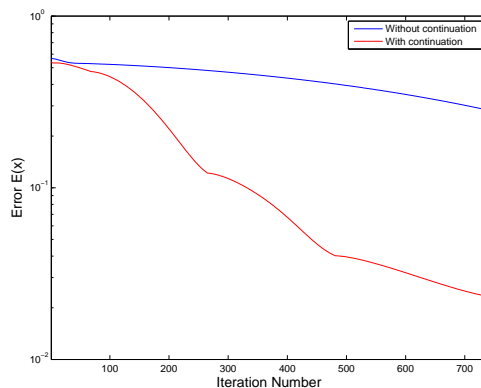


Fig. 5: Convergence comparison between SFISTA with and without continuation.

We tested the algorithm on the Shepp Logan image from the previous subsection with the same setting, using SFISTA with  $\mu_f = 10^{-4}$  and standard SFISTA with  $\mu = 10^{-4}$ . In Figure 5, we plot the reconstruction error for these two algorithms. As can be seen, continuation helps speed up the convergence. The reconstructed Shepp Logan phantom for continuation is presented in Fig. 6 with reconstruction error 2.36%.

## VI. CONCLUSION

In this paper, we proposed methods based on MFISTA to solve the analysis LASSO optimization problem. Since the proximal operator in MFISTA for  $\|\mathbf{D}^*\mathbf{x}\|_1$  does not have a closed-form solution, we presented two methods, SFISTA and DFISTA, using smoothing and decomposition respectively, to transform the original sparse recovery problem into a smooth counterpart. We analyzed the convergence of SFISTA and DFISTA and showed that SFISTA converges faster in general nonsmooth optimization problems. We also derived a bound on the performance for



Fig. 6: Reconstructed Shepp Logan with SFISTA using continuation.

both approaches assuming a tight frame and D-RIP. Our methods were demonstrated via several simulations. With the application of parameter continuation, these two algorithms are suitable to solve large scale problems.

#### APPENDIX

**Proof of Lemma IV.1:** Without loss of generality we assume that  $\|\mathbf{u}\|_2 = 1$  and  $\|\mathbf{v}\|_2 = 1$ . By the definition of D-RIP, we have

$$\begin{aligned} \operatorname{Re}\langle \mathbf{A}\mathbf{u}, \mathbf{A}\mathbf{v} \rangle &= \frac{1}{4} \{ \|\mathbf{A}\mathbf{u} + \mathbf{A}\mathbf{v}\|_2^2 - \|\mathbf{A}\mathbf{u} - \mathbf{A}\mathbf{v}\|_2^2 \} \\ &\geq \frac{1}{4} \{ (1 - \sigma_{2s}) \|\mathbf{u} + \mathbf{v}\|_2^2 - (1 + \sigma_{2s}) \|\mathbf{u} - \mathbf{v}\|_2^2 \} \\ &= -\sigma_{2s} + \operatorname{Re}\langle \mathbf{u}, \mathbf{v} \rangle. \end{aligned}$$

Now it is easy to extend this equation to get the desired result.

**Proof of Lemma IV.2:** From the definition of  $\mathcal{T}_j$  we have

$$\|\mathbf{D}_{\mathcal{T}_j}^* \mathbf{h}\|_2 \leq s^{-\frac{1}{2}} \|\mathbf{D}_{\mathcal{T}_{j-1}}^* \mathbf{h}\|_1$$

for all  $j \geq 2$ . By summing up over  $j = 2, 3, \dots$  we can have the tail bounded as

$$\sum_{j \geq 2} \|\mathbf{D}_{\mathcal{T}_j}^* \mathbf{h}\|_2 \leq s^{-\frac{1}{2}} \sum_{j \geq 1} \|\mathbf{D}_{\mathcal{T}_j}^* \mathbf{h}\|_1 = s^{-\frac{1}{2}} \|\mathbf{D}_{\mathcal{T}_c}^* \mathbf{h}\|_1. \quad (23)$$

Now, considering the fact that  $D$  is a tight frame, i.e.,  $DD^* = I$ , and validity of the D-RIP, we have

$$\begin{aligned}
& \operatorname{Re}\langle Ah, ADD_{\mathcal{T}_0}^* h \rangle \\
&= \operatorname{Re}\langle ADD_{\mathcal{T}_0}^* h, ADD_{\mathcal{T}_0}^* h \rangle + \sum_{j \geq 2} \operatorname{Re}\langle ADD_{\mathcal{T}_j}^* h, ADD_{\mathcal{T}_0}^* h \rangle \\
&\geq (1 - \sigma_{2s}) \|DD_{\mathcal{T}_0}^* h\|_2^2 + \sum_{j \geq 2} \operatorname{Re}\langle ADD_{\mathcal{T}_j}^* h, ADD_{\mathcal{T}_0}^* h \rangle \\
&\quad + \sum_{j \geq 2} \operatorname{Re}\langle ADD_{\mathcal{T}_j}^* h, ADD_{\mathcal{T}_1}^* h \rangle
\end{aligned}$$

Using the result from Lemma IV.1, we can bound the last two terms in the above inequality; hence, we derive

$$\begin{aligned}
& \operatorname{Re}\langle Ah, ADD_{\mathcal{T}_0}^* h \rangle \\
&\geq (1 - \sigma_{2s}) \|DD_{\mathcal{T}_0}^* h\|_2^2 + \sum_{j \geq 2} \operatorname{Re}\langle DD_{\mathcal{T}_j}^* h, DD_{\mathcal{T}_0}^* h \rangle \\
&\quad + \sum_{j \geq 2} \operatorname{Re}\langle DD_{\mathcal{T}_j}^* h, DD_{\mathcal{T}_1}^* h \rangle \\
&\quad - \sigma_{2s} \|DD_{\mathcal{T}_0}^* h\|_2 \sum_{j \geq 2} \|DD_{\mathcal{T}_j}^* h\|_2 \\
&\quad - \sigma_{2s} \|DD_{\mathcal{T}_1}^* h\|_2 \sum_{j \geq 2} \|DD_{\mathcal{T}_j}^* h\|_2 \\
&= (1 - \sigma_{2s}) \|DD_{\mathcal{T}_0}^* h\|_2^2 + \operatorname{Re}\left\langle \sum_{j \geq 2} DD_{\mathcal{T}_j}^* h, DD_{\mathcal{T}_0}^* h \right\rangle \\
&\quad - \sigma_{2s} (\|DD_{\mathcal{T}_0}^* h\|_2 + \|DD_{\mathcal{T}_1}^* h\|_2) \sum_{j \geq 2} \|DD_{\mathcal{T}_j}^* h\|_2
\end{aligned} \tag{24}$$

We have

$$\begin{aligned}
\operatorname{Re}\left\langle \sum_{j \geq 2} DD_{\mathcal{T}_j}^* h, DD_{\mathcal{T}_0}^* h \right\rangle &= \operatorname{Re}\langle h - DD_{\mathcal{T}_0}^* h, DD_{\mathcal{T}_0}^* h \rangle \\
&= \|D_{\mathcal{T}_0}^* h\|_2^2 - \|DD_{\mathcal{T}_0}^* h\|_2^2.
\end{aligned}$$

Combining this equation with (24) results in

$$\begin{aligned}
& \operatorname{Re}\langle Ah, ADD_{\mathcal{T}_0}^* h \rangle \\
&\geq \|DD_{\mathcal{T}_0}^* h\|_2^2 - \sigma_{2s} \|DD_{\mathcal{T}_0}^* h\|_2^2 + \|D_{\mathcal{T}_0}^* h\|_2^2 - \|DD_{\mathcal{T}_0}^* h\|_2^2 \\
&\quad - \sigma_{2s} (\|DD_{\mathcal{T}_0}^* h\|_2 + \|DD_{\mathcal{T}_1}^* h\|_2) \sum_{j \geq 2} \|DD_{\mathcal{T}_j}^* h\|_2.
\end{aligned}$$

Using the fact that when  $D$  is a tight frame,  $\|DD_{\mathcal{T}_0}^* h\|_2 \leq \|D_{\mathcal{T}_0}^* h\|_2$ , we have

$$\begin{aligned}
& \operatorname{Re}\langle Ah, ADD_{\mathcal{T}_0}^* h \rangle \\
&\geq (1 - \sigma_{2s}) \|D_{\mathcal{T}_0}^* h\|_2^2 - \sigma_{2s} (\|D_{\mathcal{T}_0}^* h\|_2 + \|D_{\mathcal{T}_1}^* h\|_2) \sum_{j \geq 2} \|D_{\mathcal{T}_j}^* h\|_2.
\end{aligned}$$

Since  $\|D_{\mathcal{T}_0}^* \mathbf{h}\|_2 + \|D_{\mathcal{T}_1}^* \mathbf{h}\|_2 \leq \sqrt{2} \|D_{\mathcal{T}_{01}}^* \mathbf{h}\|_2$  (because  $\mathcal{T}_0$   $\mathcal{T}_1$  are disjoint), we conclude that

$$\begin{aligned} & \operatorname{Re}\langle \mathbf{A}\mathbf{h}, \mathbf{A}D_{\mathcal{T}_{01}}^* \mathbf{h} \rangle \\ & \geq (1 - \sigma_{2s}) \|D_{\mathcal{T}_{01}}^* \mathbf{h}\|_2^2 - \sqrt{2}\sigma_{2s} \|D_{\mathcal{T}_{01}}^* \mathbf{h}\|_2 \sum_{j \geq 2} \|D_{\mathcal{T}_j}^* \mathbf{h}\|_2, \end{aligned}$$

which along with inequality (23) yields the desired result given by

$$\begin{aligned} & \operatorname{Re}\langle \mathbf{A}\mathbf{h}, \mathbf{A}D_{\mathcal{T}_{01}}^* \mathbf{h} \rangle \\ & \geq (1 - \sigma_{2s}) \|D_{\mathcal{T}_{01}}^* \mathbf{h}\|_2^2 - \sqrt{2}s^{-\frac{1}{2}}\sigma_{2s} \|D_{\mathcal{T}_{01}}^* \mathbf{h}\|_2 \|D_{\mathcal{T}^c}^* \mathbf{h}\|_1. \end{aligned}$$

**Proof of Lemma IV.3:** The subgradient optimality condition for RALASSO can be stated as

$$\mathbf{A}^*(\mathbf{A}\mathbf{x}_{\text{opt}} - \mathbf{b}) + \rho \mathbf{D}(\mathbf{D}^* \mathbf{x}_{\text{opt}} - \mathbf{z}_{\text{opt}}) = 0, \text{ and} \quad (25)$$

$$\lambda \mathbf{v} + \rho(\mathbf{z}_{\text{opt}} - \mathbf{D}^* \mathbf{x}_{\text{opt}}) = 0, \quad (26)$$

where  $\mathbf{v}$  is a subgradient of the function  $\|\mathbf{z}\|_1$  and consequently  $\|\mathbf{v}\|_\infty \leq 1$ . Combining (25) and (26), we have

$$\mathbf{A}^*(\mathbf{A}\mathbf{x}_{\text{opt}} - \mathbf{b}) = \lambda \mathbf{D}\mathbf{v}.$$

Multiplying both sides by  $\mathbf{D}^* \mathbf{A}^*$ , we get

$$\begin{aligned} & \|\mathbf{D}^* \mathbf{A}^*(\mathbf{A}\mathbf{x}_{\text{opt}} - \mathbf{b})\|_\infty \\ & = \lambda \|\mathbf{D}^* \mathbf{D}\mathbf{v}\|_\infty \leq \lambda \|\mathbf{D}^* \mathbf{D}\|_{\infty, \infty} = \lambda \|\mathbf{D}^* \mathbf{D}\|_{1,1}. \end{aligned} \quad (27)$$

The first inequality follows from the fact that  $\|\mathbf{v}\|_\infty \leq 1$ . With the assumption that  $\|\mathbf{D}^* \mathbf{A}^* \mathbf{w}\|_\infty \leq \frac{\lambda}{2}$ , and the triangle inequality, we have

$$\begin{aligned} & \|\mathbf{D}^* \mathbf{A}^* \mathbf{A}\mathbf{h}\|_\infty \\ & \leq \|\mathbf{D}^* \mathbf{A}^*(\mathbf{A}\mathbf{x} - \mathbf{b})\|_\infty + \|\mathbf{D}^* \mathbf{A}^*(\mathbf{A}\mathbf{x}_{\text{opt}} - \mathbf{b})\|_\infty \\ & \leq \left( \frac{1}{2} + \|\mathbf{D}^* \mathbf{D}\|_{1,1} \right) \lambda. \end{aligned} \quad (28)$$

**Proof of Lemma IV.4:** Since  $\mathbf{x}_{\text{opt}}$  and  $\mathbf{z}_{\text{opt}}$  solve the optimization problem RALASSO, we have,

$$\begin{aligned} & \frac{1}{2} \|\mathbf{A}\mathbf{x}_{\text{opt}} - \mathbf{b}\|_2^2 + \lambda \|\mathbf{z}_{\text{opt}}\|_1 + \frac{1}{2} \rho \|\mathbf{D}^* \mathbf{x}_{\text{opt}} - \mathbf{z}_{\text{opt}}\|_2^2 \\ & \leq \frac{1}{2} \|\mathbf{A}\mathbf{x} - \mathbf{b}\|_2^2 + \lambda \|\mathbf{D}^* \mathbf{x}\|_1. \end{aligned}$$

Since  $\mathbf{b} = \mathbf{A}\mathbf{x} + \mathbf{w}$  and  $\mathbf{h} = \mathbf{x}_{\text{opt}} - \mathbf{x}$ , it follows that

$$\begin{aligned} & \frac{1}{2} \|\mathbf{A}\mathbf{h} - \mathbf{w}\|_2^2 + \lambda \|\mathbf{z}_{\text{opt}}\|_1 + \frac{1}{2} \rho \|\mathbf{D}^* \mathbf{x}_{\text{opt}} - \mathbf{z}_{\text{opt}}\|_2^2 \\ & \leq \frac{1}{2} \|\mathbf{w}\|_2^2 + \lambda \|\mathbf{D}^* \mathbf{x}\|_1. \end{aligned}$$

Expanding and rearranging the terms in the above equation, we get

$$\begin{aligned} & \frac{1}{2}\|\mathbf{A}\mathbf{h}\|_2^2 + \lambda\|\mathbf{z}_{\text{opt}}\|_1 + \frac{1}{2}\rho\|\mathbf{D}^*\mathbf{x}_{\text{opt}} - \mathbf{z}_{\text{opt}}\|_2^2 \\ & \leq \text{Re}\langle \mathbf{A}\mathbf{h}, \mathbf{w} \rangle + \lambda\|\mathbf{D}^*\mathbf{x}\|_1, \end{aligned}$$

Using the equation (26) to replace the terms with  $\mathbf{z}_{\text{opt}}$ , we have

$$\begin{aligned} & \frac{1}{2}\|\mathbf{A}\mathbf{h}\|_2^2 + \lambda\left\|\mathbf{D}^*\mathbf{x}_{\text{opt}} - \frac{\lambda}{\rho}\mathbf{v}\right\|_1 + \frac{1}{2}\rho\left\|\frac{\lambda}{\rho}\mathbf{v}\right\|_2^2 \\ & \leq \text{Re}\langle \mathbf{A}\mathbf{h}, \mathbf{w} \rangle + \lambda\|\mathbf{D}^*\mathbf{x}\|_1. \end{aligned}$$

Using the fact that  $\|\mathbf{D}^*\mathbf{x}_{\text{opt}} - \frac{\lambda}{\rho}\mathbf{v}\|_1 \geq \|\mathbf{D}^*\mathbf{x}_{\text{opt}}\|_1 - \frac{\lambda}{\rho}\|\mathbf{v}\|_1$ , we have

$$\begin{aligned} & \frac{1}{2}\|\mathbf{A}\mathbf{h}\|_2^2 + \lambda\|\mathbf{D}^*\mathbf{x}_{\text{opt}}\|_1 \\ & \leq \frac{\lambda^2}{\rho}\|\mathbf{v}\|_1 - \frac{\lambda^2}{2\rho}\|\mathbf{v}\|_2^2 + \text{Re}\langle \mathbf{A}\mathbf{h}, \mathbf{w} \rangle + \lambda\|\mathbf{D}^*\mathbf{x}\|_1 \\ & \leq \frac{\lambda^2 p}{2\rho} + \text{Re}\langle \mathbf{A}\mathbf{h}, \mathbf{w} \rangle + \lambda\|\mathbf{D}^*\mathbf{x}\|_1. \end{aligned} \tag{29}$$

The second inequality follows from the fact that  $\frac{\lambda^2}{\rho}\|\mathbf{v}\|_1 - \frac{\lambda^2}{2\rho}\|\mathbf{v}\|_2^2$  is maximized when every element of  $\mathbf{v} \in \mathbb{R}^p$  is 1. Now, with the assumption that  $\mathbf{D}$  is a tight frame, we have the following relation,

$$\begin{aligned} \text{Re}\langle \mathbf{A}\mathbf{h}, \mathbf{w} \rangle + \lambda\|\mathbf{D}^*\mathbf{x}\|_1 & = \text{Re}\langle \mathbf{D}^*\mathbf{h}, \mathbf{D}^*\mathbf{A}^*\mathbf{w} \rangle + \lambda\|\mathbf{D}^*\mathbf{x}\|_1 \\ & \leq \|\mathbf{D}^*\mathbf{h}\|_1 \|\mathbf{D}^*\mathbf{A}^*\mathbf{w}\|_\infty + \lambda\|\mathbf{D}^*\mathbf{x}\|_1. \end{aligned}$$

The first inequality follows from the fact that  $\text{Re}\langle \mathbf{x}, \mathbf{y} \rangle \leq \|\langle \mathbf{x}, \mathbf{y} \rangle\| \leq \|\mathbf{x}\|_1 \|\mathbf{y}\|_\infty$ . Using the assumption that  $\|\mathbf{D}^*\mathbf{A}^*\mathbf{w}\|_\infty \leq \frac{\lambda}{2}$ , we get

$$\text{Re}\langle \mathbf{A}\mathbf{h}, \mathbf{w} \rangle + \lambda\|\mathbf{D}^*\mathbf{x}\|_1 \leq \frac{\lambda}{2}\|\mathbf{D}^*\mathbf{h}\|_1 + \lambda\|\mathbf{D}^*\mathbf{x}\|_1. \tag{30}$$

Now, using the results from inequalities (29) and (30), we have

$$\begin{aligned} \lambda\|\mathbf{D}^*\mathbf{x}_{\text{opt}}\|_1 & \leq \frac{1}{2}\|\mathbf{A}\mathbf{h}\|_2^2 + \lambda\|\mathbf{D}^*\mathbf{x}_{\text{opt}}\|_1 \\ & \leq \frac{\lambda^2}{2\rho}p + \text{Re}\langle \mathbf{A}\mathbf{h}, \mathbf{w} \rangle + \lambda\|\mathbf{D}^*\mathbf{x}\|_1 \\ & \leq \frac{\lambda^2}{2\rho}p + \frac{\lambda}{2}\|\mathbf{D}^*\mathbf{h}\|_1 + \lambda\|\mathbf{D}^*\mathbf{x}\|_1, \end{aligned}$$

which is the same as,

$$\|\mathbf{D}^*\mathbf{x}_{\text{opt}}\|_1 \leq \frac{\lambda}{2\rho}p + \frac{1}{2}\|\mathbf{D}^*\mathbf{h}\|_1 + \|\mathbf{D}^*\mathbf{x}\|_1.$$

Since we have  $\mathbf{h} = \mathbf{x}_{\text{opt}} - \mathbf{x}$ , it follows that

$$\|\mathbf{D}^*\mathbf{h} + \mathbf{D}^*\mathbf{x}\|_1 \leq \frac{\lambda}{2\rho}p + \frac{1}{2}\|\mathbf{D}^*\mathbf{h}\|_1 + \|\mathbf{D}^*\mathbf{x}\|_1,$$



and hence

$$\begin{aligned} & \|D_{\mathcal{T}}^* \mathbf{h} + D_{\mathcal{T}}^* \mathbf{x}\|_1 + \|D_{\mathcal{T}^c}^* \mathbf{h} + D_{\mathcal{T}^c}^* \mathbf{x}\|_1 \\ & \leq \frac{\lambda}{2\rho} p + \frac{1}{2} \|D_{\mathcal{T}}^* \mathbf{h}\|_1 + \frac{1}{2} \|D_{\mathcal{T}^c}^* \mathbf{h}\|_1 + \|D_{\mathcal{T}}^* \mathbf{x}\|_1 + \|D_{\mathcal{T}^c}^* \mathbf{x}\|_1. \end{aligned}$$

Applying the triangle inequality to the left handside of above inequality, we have

$$\begin{aligned} & - \|D_{\mathcal{T}}^* \mathbf{h}\|_1 + \|D_{\mathcal{T}}^* \mathbf{x}\|_1 + \|D_{\mathcal{T}^c}^* \mathbf{h}\|_1 - \|D_{\mathcal{T}^c}^* \mathbf{x}\|_1 \\ & \leq \frac{\lambda}{2\rho} p + \frac{1}{2} \|D_{\mathcal{T}}^* \mathbf{h}\|_1 + \frac{1}{2} \|D_{\mathcal{T}^c}^* \mathbf{h}\|_1 + \|D_{\mathcal{T}}^* \mathbf{x}\|_1 + \|D_{\mathcal{T}^c}^* \mathbf{x}\|_1. \end{aligned}$$

After rearranging the terms, we have the following cone constraint,

$$\|D_{\mathcal{T}^c}^* \mathbf{h}\|_1 \leq \frac{\lambda}{\rho} p + 3\|D_{\mathcal{T}}^* \mathbf{h}\|_1 + 4\|D_{\mathcal{T}^c}^* \mathbf{x}\|_1. \quad (31)$$

#### REFERENCES

- [1] E. Candès and M. Wakin, “An introduction to compressive sampling,” *IEEE Signal Process. Mag.*, vol. 25, no. 2, pp. 21–30, Mar. 2008.
- [2] E. Candès, J. Romberg, and T. Tao, “Robust uncertainty principles: exact signal reconstruction from highly incomplete frequency information,” *IEEE Trans. Inf. Theory*, vol. 52, no. 2, pp. 489–509, Feb. 2006.
- [3] E. Candès and T. Tao, “Near-optimal signal recovery from random projections: Universal encoding strategies?” *IEEE Trans. Inf. Theory*, vol. 52, no. 12, pp. 5406–5425, Dec. 2006.
- [4] Y. C. Eldar and G. Kutyniok, *Compressed Sensing: Theory and Applications*. Cambridge University Press, 2012.
- [5] T. Blumensath and M. E. Davies, “Iterative hard thresholding for compressed sensing,” *Applied and Computational Harmonic Analysis*, vol. 27, no. 3, pp. 265–274, 2009. [Online]. Available: <http://www.sciencedirect.com/science/article/pii/S1063520309000384>
- [6] J. Tropp and A. Gilbert, “Signal recovery from random measurements via orthogonal matching pursuit,” *IEEE Trans. Inf. Theory*, vol. 53, no. 12, pp. 4655–4666, Dec. 2007.
- [7] D. S.S.Chen and M.A.Saunders, “Atomic decomposition by basis pursuit,” *SIAM Rev.*, vol. 43, no. 3, pp. 129–159, Mar. 2001.
- [8] R. T. T. Hastie and J. Friedman, *The Elements of Statistical Learning: Data, Mining, Intereference, and Prediction, 2nd ed.* New York: Springer, 2009.
- [9] E. Candès, “The restricted isometry property and its implications for compressed sensing,” *C. R. Acad. Sci. Paris, Ser. I*, 2008.
- [10] P. Bickel, Y. Ritov, and A. Tsybakov, “Simultaneous analysis of lasso and dantzig selector,” *Ann. Statist.*, 2009.
- [11] T. Blumensath and M. Davies, “Normalized iterative hard thresholding: Guaranteed stability and performance,” *IEEE J. Sel. Topics Signal Process.*, vol. 4, no. 2, pp. 298–309, 2010.
- [12] E. J. Candès, Y. C. Eldar, D. Needell, and P. Randall, “Compressed sensing with coherent and redundant dictionaries,” *Appl. Comput. Harmon. Anal.*, 2011.
- [13] S. Nam, M. Davies, M. Elad, and R. Gribonval, “The cospase analysis model and algorithms,” *Applied and Computational Harmonic Analysis*, vol. 34, no. 1, pp. 30–56, 2013. [Online]. Available: <http://www.sciencedirect.com/science/article/pii/S1063520312000450>
- [14] T. Peleg and M. Elad, “Performance guarantees of the thresholding algorithm for the cospase analysis model,” *IEEE Trans. Ind. Informat.*, vol. 59, no. 3, pp. 1832–1845, 2013.
- [15] R. Giryes, S. Nam, M. Elad, R. Gribonval, and M. Davies, “Greedy-like algorithms for the cospase analysis model,” *Linear Algebra and its Applications*, no. 0, pp. –, 2013. [Online]. Available: <http://www.sciencedirect.com/science/article/pii/S0024379513001870>
- [16] S. Boyd and L. Vandenberghe, *Convex Optimization*. Cambridge University Press, 2004.
- [17] S. Boyd, N. Parikh, E. Chu, B. Peleato, and J. Eckstein, “Distributed optimization and statistical learning via alternating direction method of multipliers,” in *Found. Trends Mach Learning*, vol. 3, 2010, pp. 1–122.
- [18] M. Afonso, J. Bioucas-Dias, and M. A. T. Figueiredo, “Fast image recovery using variable splitting and constrained optimization,” *IEEE Trans. Image Process.*, vol. 19, no. 9, pp. 2345–2356, 2010.

- [19] A. Beck and M. Teboulle, “Fast gradient-based algorithms for constrained total variation image denoising and deblurring problems,” *IEEE Trans. Image Process.*, vol. 18, no. 11, pp. 2419–2434, Nov.
- [20] —, “Smoothing and first order methods: a unified framework,” *SIAM J. Optim.*, vol. 22, no. 2, pp. 557–580, 2012.
- [21] S. Becker, J. Bobin, and E. J. Candès, “Nesta: a fast and accurate first-order method for sparse recovery,” *SIAM J. on Imaging Sciences* 4(1), pp. 1–39.
- [22] Y. Nesterov, “Smooth minimization of non-smooth functions,” *Math. Program.*, vol. 103, no. 1, pp. 127–152, 2005.
- [23] R. Courant, “Variational methods for the solution of problems with equilibrium and vibration,” *Bull. Amer. Math. Soc.*, vol. 49, pp. 1–23, 1943.
- [24] Y. Wang, J. Yang, W. Yin, and Y. Zhang, “A new alternating minimization algorithm for total variation image reconstruction,” *SIAM J. Imaging Sciences*, vol. 1, no. 3, pp. 248–272, 2008.
- [25] S. Li and J. Lin, “Compressed sensing with coherent tight frames via  $l_q$ -minimization for  $0 < q \leq 1$ ,” *arXiv:1105.3299*.
- [26] J. Lin and S. Li, “Sparse recovery with coherent tight frame via analysis dantzig selector and analysis lasso,” *arXiv:1301.3248*.
- [27] D. Needell and J. Tropp, “Cosamp: Iterative signal recovery from noisy samples,” *Appl. Comput. Harmon. Anal.*, vol. 26, no. 3, pp. 301–321, 2008.
- [28] J. J. Moreau, “Proximité et dualité dans un espace hilbertien,” *Bull. Soc. Math. France*, vol. 93, pp. 273–299, 1965.
- [29] P. Combettes and V. Wajs, “Signal recovery by proximal forward-backward splitting,” *Multiscale Modeling and Simulation*, vol. 4, pp. 1168–1200, 2005.
- [30] A. Beck and M. Teboulle, “A fast iterative shrinkage-thresholding algorithm for linear inverse problems,” *SIAM. on Imaging Sciences* 2(1), 2009.
- [31] —, “Gradient-based algorithms with applications to signal recovery problems,” in *Convex Optimization in Signal Processing and Communications*, D. Palomar and Y. Eldar, Eds. Cambridge University Press, 2009, pp. 139–162.
- [32] Y. E. Nesterov, “A method for solving the convex programming problem with convergence rate  $O(1/k^2)$ ,” *Dokl. Akad. Nauk SSSR*, vol. 269, no. 3, pp. 543–547, 1983.
- [33] P. J. Huber, “Robust estimation of a location parameter,” *Ann. Math. Statist.*, vol. 35, pp. 73–101, 1964.
- [34] M. A. T. Figueiredo, R. Nowak, and S. Wright, “Gradient projection for sparse reconstruction: Application to compressed sensing and other inverse problems,” *Selected Topics in Signal Processing, IEEE Journal of*, vol. 1, no. 4, pp. 586–597, 2007.